AN ABSTRACT OF THE THESIS OF

Leonard Thomas Elliott for the Master of Science in
(Name) (Degree)

Mechanical Engineering
(Major)

Date thesis is presented October 3, 1963

Title: CATASTROPHIC PROPAGATION OF DUCTILE CRACKS IN METALLIC FOILS.

Abstract Approved: Redacted for Privacy

The sudden failure of metal structures under load, which has been a design problem for many years, is characterized by a crack propagation rate which approaches the speed of sound in the material. These failures, which are often known as catastrophic fractures, may be divided into two types which depend on the particular material in question. Fractures which cause a very small amount of plastic deformation associated with low energy absorption are known as brittle fractures, whereas high energy absorption during fracture, due to large amounts of plastic deformation, is associated with ductile fracture.

The Griffith theory for spontaneous fracture in brittle materials states that the strain energy released during fracture must be greater than the energy needed to form the new crack surface area. This theory, which has been verified experimentally for brittle materials, is not applicable to ductile materials since the energy of plastic

deformation during crack propagation must be taken into account. The revised and simplified theory for ductile materials states that the strain energy must exceed the energy needed to cause plastic deformation ahead of the crack. The steps in the fracture of ductile materials are initiation, slow crack growth, and rapid or catastrophic crack propagation, and the variable plastic deformation involved in these steps causes the process to be complex in behavior and analysis. However, an understanding of the causes of slow and rapid crack growth can be obtained by studying the effects of plastic deformation at the tip of a propagating crack.

The objective of this thesis was to investigate the factors which affect the tendency for a ductile crack to propagate catastrophically. This was accomplished through the use of two types of investigations. In the first investigation an attempt was made to obtain catastrophic failure in 18 x 32 inch uniaxially stressed sheets of commercial household aluminum foil by introducing a crack in the center of the sheet in such a manner that the crack was elongated outwards in each direction. The catastrophic failure which was observed, however, was due to the addition of extra energy to the system boundaries which was not accounted for in the theory. Slow crack propagation was also observed and led to the second investigation.

The plastic deformation at the crack tip was studied by visual observation using a metallograph and by actual measurement of the amount of deformation occurring during crack growth. This was done

with a Tukon microhardness tester in which indentations were placed on the foil specimens, which were later given a small crack at the center, and which were mounted in a drill press vice on the tester. The crack was then propagated by turning the screw on the vice and measurements of the deformation between the indentations were made.

The photographs and measurements of the plastic deformation at the crack tip showed that deformation existed throughout the entire specimen and was not localized in a given area at the crack tip as has been assumed in some theories. The existance of elastic strain in the material was shown by the occurrence of elastic recovery in the strain relieved areas of the cracked material although no differentiation could be made between the area of elastic and plastic deformation. The existance of a stable configuration of iso-strain contours surrounding the tip of the crack was also shown.

Calculations of the strain energy needed to satisfy the plastic deformation energy requirements showed that a crack length of about 49 inches would be needed to cause catastrophic failure. This is much larger than the specimen size used and would explain the lack of rapid crack growth in the tests run under near theoretical conditions.

CATASTROPHIC PROPAGATION OF DUCTILE CRACKS IN METALLIC FOILS

by

LEONARD THOMAS ELLIOTT

A THESIS

submitted to

OREGON STATE UNIVERSITY

in partial fulfillment of
the requirements for the
degree of

MASTER OF SCIENCE

June 1964

APPROVED:

Redacted for Privacy

Associate Professor of Mechanical Engineering

Redacted for Privacy

Head of Department Mechanical and Industrial Engineering

Redacted for Privacy

Dean of Graduate School

Date thesis is presented October 3, 1963

Typed by Joan Shaw

ACKNOWLEDGEMENTS

The author wishes to express his appreciation and gratitude to Professor R. D. Olleman of the Department of Mechanical Engineering for his encouragement and advice during the design and testing of the equipment involved in this project and for his subsequent help in the correlation of the data obtained and in the preparation of the thesis.

The author also wishes to thank Professor O. G. Paasche of the Department of Mechanical Engineering for his technical advice and assistance in the construction of the experimental equipment.

TABLE OF CONTENTS

LIST OF FIGURES

LIST OF TABLES

NOMENCLATURE

C	Half Crack Length
S	Specific Surface Energy
E	Modulus of Elasticity
K	Kinetic Energy
P	Work Done in Plastic Deformation
G	Strain Energy
A	Surface Area of Crack
h	Distance Between Boundary Clamps
K_1	Constant $-\pi/2$
K_2	Constant - 1
t	Thickness of the Sheet
ℓ	Length of the Crack
x	Work done on Boundaries
σ	Stress - psi
σ_c	Critical Stress - psi
σ_f	Fracture Stress - psi

CATASTROPHIC PROPAGATION OF DUCTILE CRACKS IN METALLIC FOILS

INTRODUCTION

The problem of fracture in metals has been well known ever since the first implements were fabricated thousands of years ago. It is only recently, however, that any sort of understanding has been attained of the processes that occur during the fracturing of a metal structure. Even now, a great deal of confusion is associated with the causes of the various types of fracture that occur and the relationships between these causes.

Catastrophic Crack Propagation

It is generally noted that there are two basic types of fracture, brittle and ductile, which are associated with the various types of materials. It has been found, however, that one type of fracture is not necessarily associated with one given material. Instead, some materials are capable of fracturing either in a ductile or a brittle manner depending on the particular material and on the external conditions such as the loading rate, stress concentrations, and temperature of the material. This ductile-to-brittle transition in the properties of a material is of extreme importance and is of particular concern in structural steels.

The graph in Figure 1 shows the transition of a structural steel from ductile to brittle as the temperature of testing decreases.

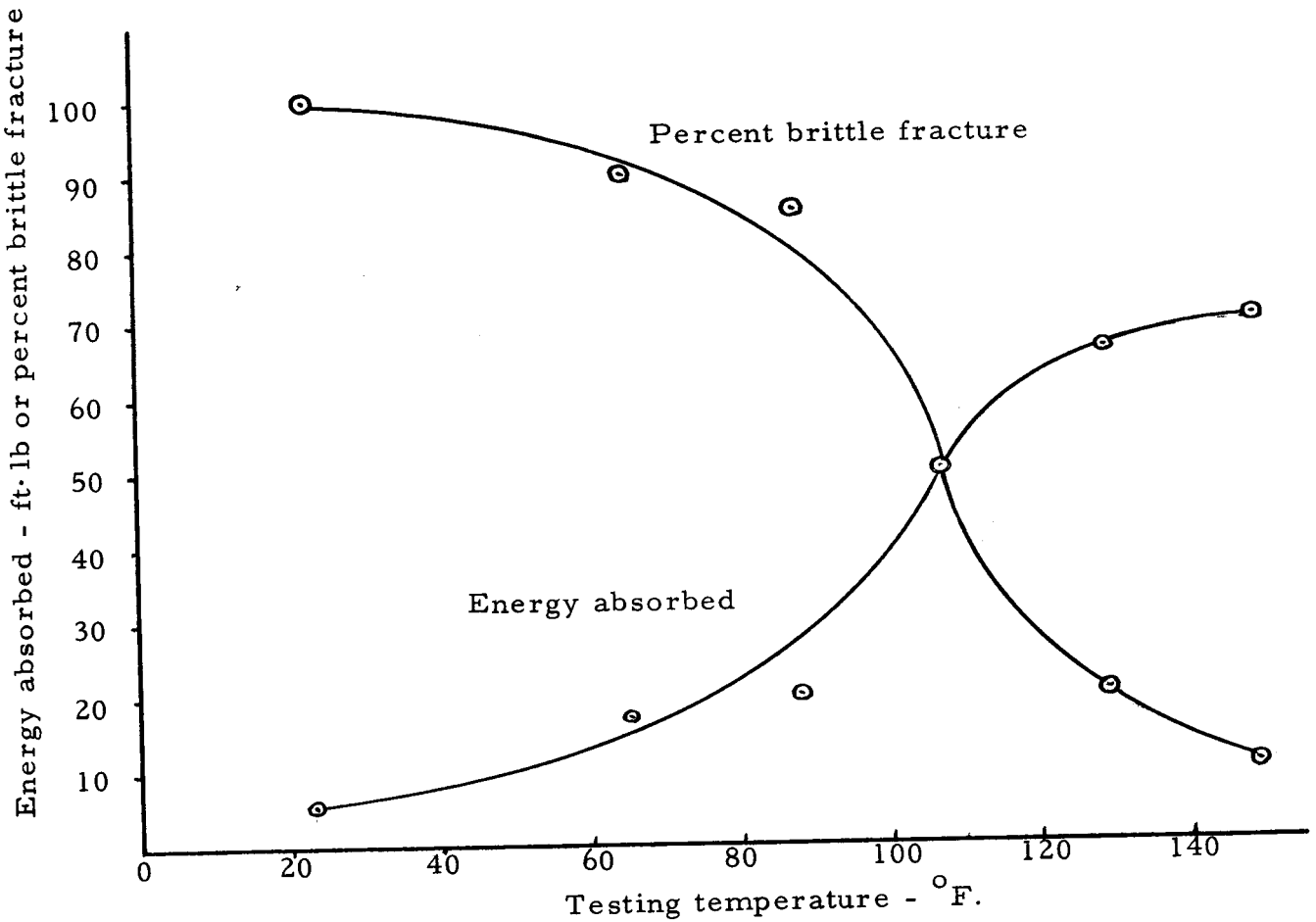

Fig. 1. Ductile-to-Brittle Transition of Structural Steel with Changing Temperature.

These data were obtained from Charpy impact tests in which small, notched specimens of a material are subjected to impact bending. It is seen that the energy absorption ability of the material decreased as the testing temperature decreased.

Practical examples of the problems that this transition can cause have been seen in the failures of many steel ships. In most cases of brittle fracture the velocity of propagation of the crack approaches the speed of sound in the material. This rapid crack extension is often termed catastrophic propagation and is common in brittle materials -- materials that can fracture with the absorption of little energy.

The analysis of the causes of fractures is not, however, as simple as might be indicated in the above discussion. It has been found that ductile metals can fracture in a catastrophic manner even when they are subjected to average stresses far below the normal tensile strength of the material. This phenomenon has been observed and investigated by several other workers in the field and it forms the basis for the present investigation.

Thesis Objective

The objective of this thesis was to make a general investigation of the factors which affect the tendency for a crack in a ductile material to propagate in a catastrophic manner.

LITERATURE REVIEW

The mathematical description of the phenomenon of crack propagation is one which has not as yet been clearly and completely derived. The theory behind the growth of rapid cracks is currently under investigation by many workers in the field and the primary theories have tended to divide themselves into two different schools[a], those which describe the process through the use of stress analysis at the crack tip, and those which consider the energies involved in causing the crack to propagate. Although the energy method has been called inadequate by some who are of the stress analysis school, it has certain advantages in that the satisfaction of the energy requirements is a necessary condition before propagation can take place and the energy method is probably the most widely accepted and most thoroughly developed of all the theories that have yet been proposed.

Griffith Crack Theory

In developing the theory for the rapid propagation of cracks in a ductile material it is convenient to first consider the criteria for the propagation of a crack in a brittle material as was first proposed by Griffith. This theory was verified by experiments performed on glass rods. To understand this theory consider a rectangular specimen which has a tensile stress applied to it which is insufficient to cause

fracture. An elliptical discontinuity is then introduced into the rod as shown in Figure 2. The problem is to relate the length of the crack, 2C, to the average stress necessary to extend it. The Griffith theory states that the crack will grow in length if the decrease in the elastic strain energy due to an increase in C is greater than the increase in the surface energy caused by increasing the free surface area of the crack due to elongation of the crack (8, p. 163-198).

The value of the decrease in elastic strain energy due to the formation of a crack of length 2C in a medium subjected to an average stress σ is estimated as:[1]

$$\text{Strain Energy} = \frac{\pi C^2 \sigma^2 t}{E}$$

The surface energy is given by, 4CSt, where S is the specific surface energy, and 4Ct is the crack surface area. In order for the crack to be in equilibrium the rate of the reduction in the elastic energy must equal the rate of the increase in the surface energy. Assuming the thickness, t, as unity:

$$\frac{d}{dC}\left(4CS - \frac{\pi C^2 \sigma^2}{E}\right) = 0$$

or:

$$\sigma_c = \left(\frac{2ES}{\pi C}\right)^{1/2}$$

---

[1] The table of nomenclature preceeding the Introduction contains all the symbols used in this thesis.

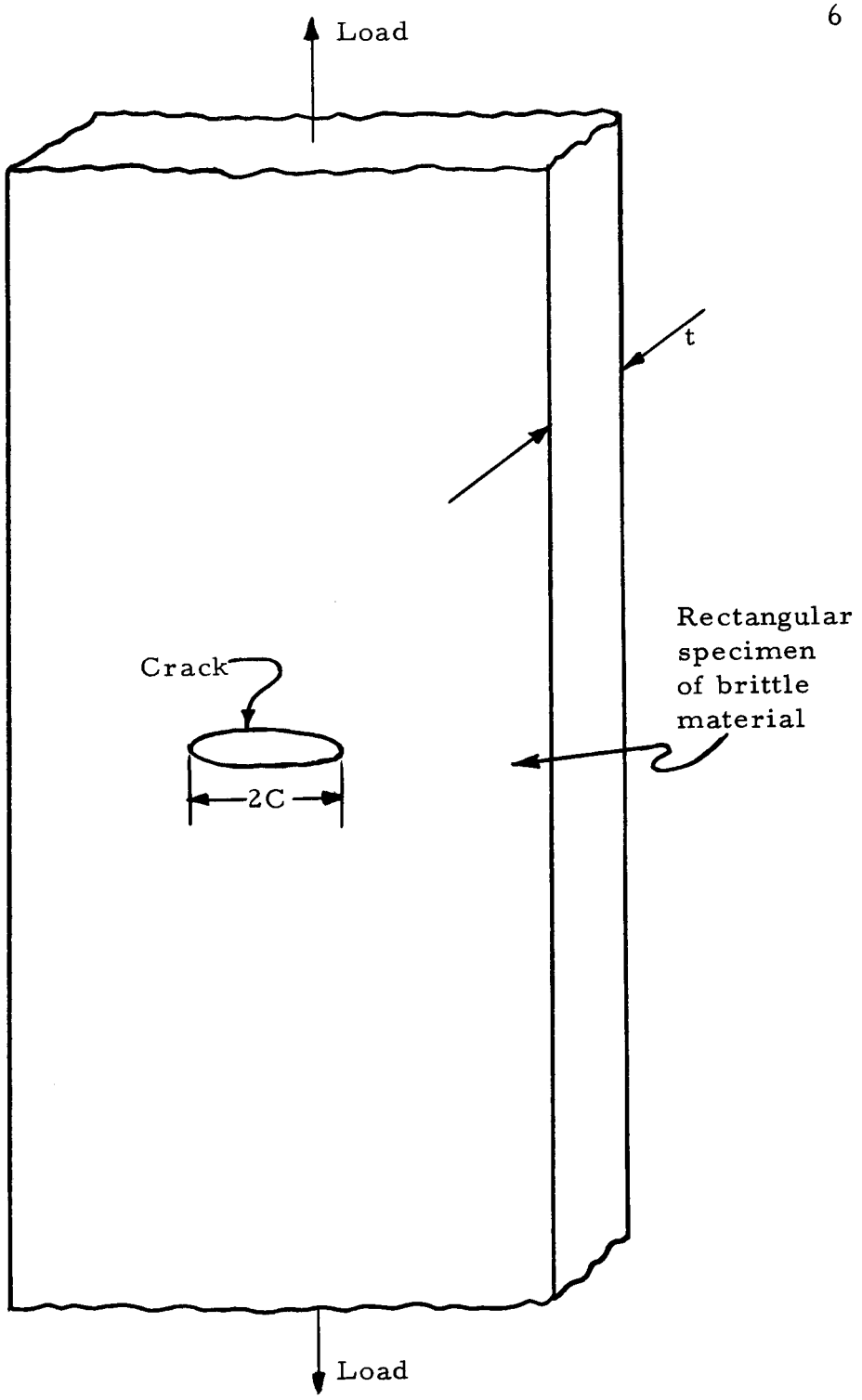

Fig. 2. Physical Situation to Which the Griffith Analysis is Applied.

Consequently, as the value of C increases, the critical value of stress decreases so that as the crack elongates the average stress required to extend it spontaneously becomes progressively less (5, p. 197).

Modification of the Griffith Theory for Ductile Materials

The Griffith theory is only applicable to completely brittle materials and hence is of little use in describing the growth of cracks in metals in which plastic deformation usually occurs. For a ductile material, the effects of plastic deformation in a thin layer of material near the crack surface on the energies involved must be considered. Orowan has shown that the addition of a plastic deformation term to the Griffith energy theory for brittle materials will describe the energy relation in a ductile fracture (13). For the ductile mode of fracture the energy equation may be written:

$$\frac{dX}{dA} + \frac{dG}{dA} = \frac{dS}{dA} + \frac{dP}{dA} + \frac{dK}{dA}$$

where:

dA = Increment of new surface that is created by an incremental extension of the crack.

$\frac{dX}{dA}$ = Rate of external work done by boundary forces loading the specimen with increases in crack surface area.

$\frac{dG}{dA}$ = Rate of strain energy released with increases in crack surface area.

$\frac{dS}{dA}$ = Rate of surface energy increase required by the material with increases in crack surface area.

$\frac{dP}{dA}$ = Rate of energy absorbed in plastic deformation with increases in crack surface area.

$\frac{dK}{dA}$ = Rate of increase in kinetic energy of the system with increases in crack surface area.

For ductile materials, Orowan has shown that dS/dA is about 10^{-4} times dP/dA and thus may be ignored (13). The energy equation then becomes:

$$\frac{dX}{dA} + \frac{dG}{dA} = \frac{dP}{dA} + \frac{dK}{dA}$$

For the purpose of comparison, the energy relation for a brittle material is:

$$\frac{dX}{dA} + \frac{dG}{dA} = \frac{dS}{dA} + \frac{dK}{dA}$$

This is a more general expression than the one already given in the discussion of brittle fracture in that the previous energy equation was for the case where the strain rate was zero and hence the work done and the kinetic energy terms were zero.

It will be noticed that the only difference in these two expressions is the interchange of dP/dA and dS/dA. For a brittle fracture dS/dA is a physical constant of the material, whereas, dP/dA for a ductile material is dependent on other variables. These include: Geometry considerations, volume of yielded material, loading conditions, and work hardening characteristic of the material.

The stability of the ductile crack is related to the rate of change of kinetic energy. The energy equations for these three states are shown below:

Stable State

$$\frac{dX}{dA} + \frac{dG}{dA} < \frac{dP}{dA} \quad \text{when} \quad \frac{dK}{dA} = 0$$

Unstable State

$$\frac{dX}{dA} + \frac{dG}{dA} > \frac{dP}{dA} \quad \text{when} \quad \frac{dK}{dA} = (+)$$

Critical State

$$\frac{dX}{dA} + \frac{dG}{dA} = \frac{dP}{dA} \quad \text{when} \quad \frac{dK}{dA} = 0$$

For the purpose of this investigation, the critical state is of the most interest since it represents the boundary between stability and instability. Therefore, the kinetic energy will not be considered in the following discussion.

Application of the Ductile Crack Theory

The terms on the left-hand side of the above equation are the energies which cause the cracking and they are dependent upon the geometry, loading conditions, and elastic properties of the material. There are two basic geometrical configurations which may be considered for a sheet of material stressed uniaxially. These are the case where the boundaries of the sheet are clamped at infinity and the case where the boundaries are clamped a finite distance from the crack. These configurations are shown in Figure 3.

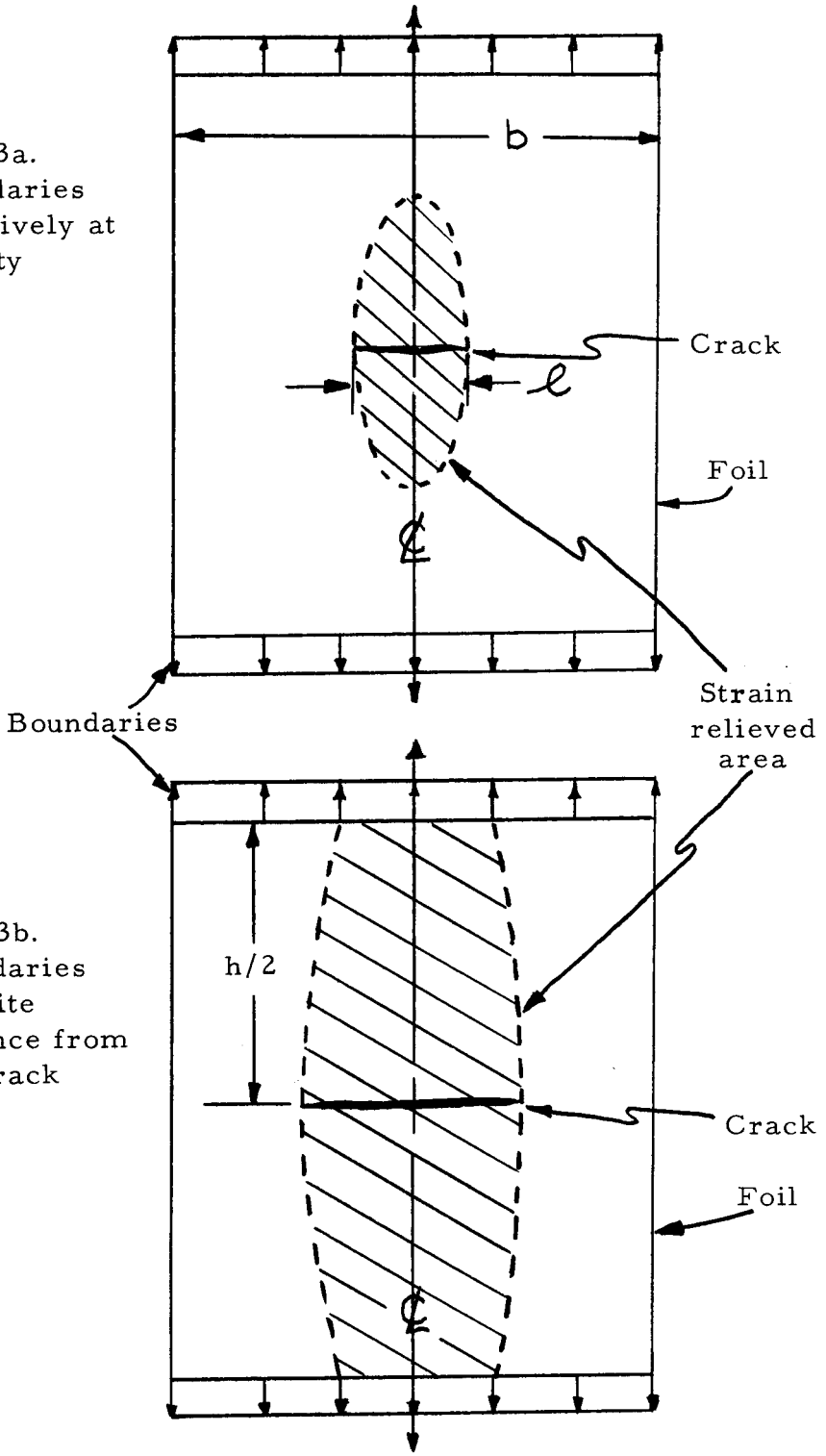

Fig. 3a. Boundaries effectively at infinity

Fig. 3b. Boundaries at finite distance from the crack

Fig. 3. Geometrical Configurations for a Crack in Foil Sheets.

For the case where the boundaries in the direction of loading are at infinity, the sheet is loaded and the loading boundaries are fixed in position so that no further energy may be supplied to the system. Therefore:

$$\frac{dX}{dA} = 0$$

The energy equation then becomes:

$$\frac{dG}{dA} = \frac{dP}{dA}$$

As the crack begins to progress, the strain energy may be visualized to be released from the shaded area in Figure 3a. This released energy is estimated as:

$$G = \frac{\sigma^2}{2E} K_1 \ell^2 t$$

where:

ℓ - Length of the crack

t - Thickness of the sheet (constant)

K_1 - A numerical constant ($K_1 = \pi / 2$)

σ - Stress applied before cracking

E - Modulus of elasticity (constant)

The new area formed per unit increase in crack length is:

$$dA = 2td\ell$$

Therefore, differentiating the expression for G:

$$\frac{dG}{dA} = \frac{dG}{d\ell} \times \frac{1}{2t} = \frac{\sigma^2}{2E} K_1 \ell$$

Instability occurs when the rate of release of strain energy, dG/dA, exceeds the rate of dissipation of plastic work, dP/dA. Experimental results have shown that dP/dA is fairly constant and for the purpose of this derivation it is assumed that this is true (14, p. B-8). At the critical crack length:

$$\frac{dP}{dA} = \frac{dG}{dA} = \frac{\sigma^2 K_1 \ell_{cr}}{2E}$$

dG/dA will increase as the crack lengthens beyond ℓ_{cr} and will then exceed dP/dA. The boundary between stable and unstable cracks is:

$$\frac{dG}{dA} = \frac{\sigma^2 K_1 \ell_{cr}}{2E}$$

This is the relation of most interest. It also provides a parameter which may be used to evaluate the effects of metallurgical variables upon the value of the critical crack length.

Consideration of the second geometrical configuration, Figure 3b, will illustrate the effects of geometry on the critical crack length. In this case the boundaries are considered to be located at a finite distance of h/2 from the crack in a sheet of width "b" where h/2 is much less than "b". As the crack lengthens, the area from which the strain energy is released is confined by the existance of the boundaries. When the crack is long enough, the strain energy becomes proportional to the first power of the crack length. The strain energy is estimated as:

$$G = \frac{\sigma^2}{2E} K_2 \ell h t$$

or:

$$\frac{dG}{dA} = \frac{\sigma^2}{4E} K_2 h$$

Applying the stability condition:

$$\frac{dP}{dA} = \frac{dG}{dA}$$

where dP/dA is constant, and dG/dA increases with "h" we obtain:

$$\frac{dG}{dA} = \frac{\sigma^2}{4E} K_2 h_{cr}$$

Therefore, the critical crack length criterion is replaced by a critical boundary spacing criterion. It is important to note that in both cases the basic criterion for crack stability is the rate of release of stored energy (14, p. 13).

For any particular set of test conditions, criticality may be determined by the crack length or by the boundary spacing and in some cases by both. In order to understand this phenomenon it is convenient to consider the effect of "ℓ" and "h/2" on the value of dG/dA. This may be done by plotting a graph of dG/dA for various values of ℓ. From the equation in which the boundaries are considered to be at infinity:

$$\frac{dG}{dA} = \frac{\sigma^2}{2E} K_1 \ell$$

it can be seen that there is a linear relationship between dG/dA and ℓ.

When this is plotted for various values of stress there will result a series of straight lines passing through the origin. Each line will represent a different value of stress. These are shown by the sloping lines in Figure 4.

From the criterion for criticality:

$$\frac{dP}{dA} = \frac{dG}{dA}$$

it can be seen that there is a value of dG/dA at which criticality occurs. Therefore, for any given value of stress the crack length can be increased until the critical value of dG/dA is reached at which point the crack propagates catastrophically.

As the boundary spacing is decreased, the situation becomes increasingly complex. As has been previously pointed out, the effect of decreasing "h/2" is to cause the boundary clamps to intersect the strain relieved area. This in turn affects the energy that is available for crack propagation. In the case where h/2 is much less than the width of the sheet, the relation involving dG/dA is:

$$\frac{dG}{dA} = \frac{\sigma^2 K_{2h}}{4E}$$

As can be seen, the crack length has no effect on the value of dG/dA. Hence, for a given stress condition the value of h/2 corresponding to the different values of dG/dA can be calculated. When this is done, a series of lines parallel to the abcissa may be drawn. This is shown by the horizontal lines in Figure 4. Since the criterion for instability

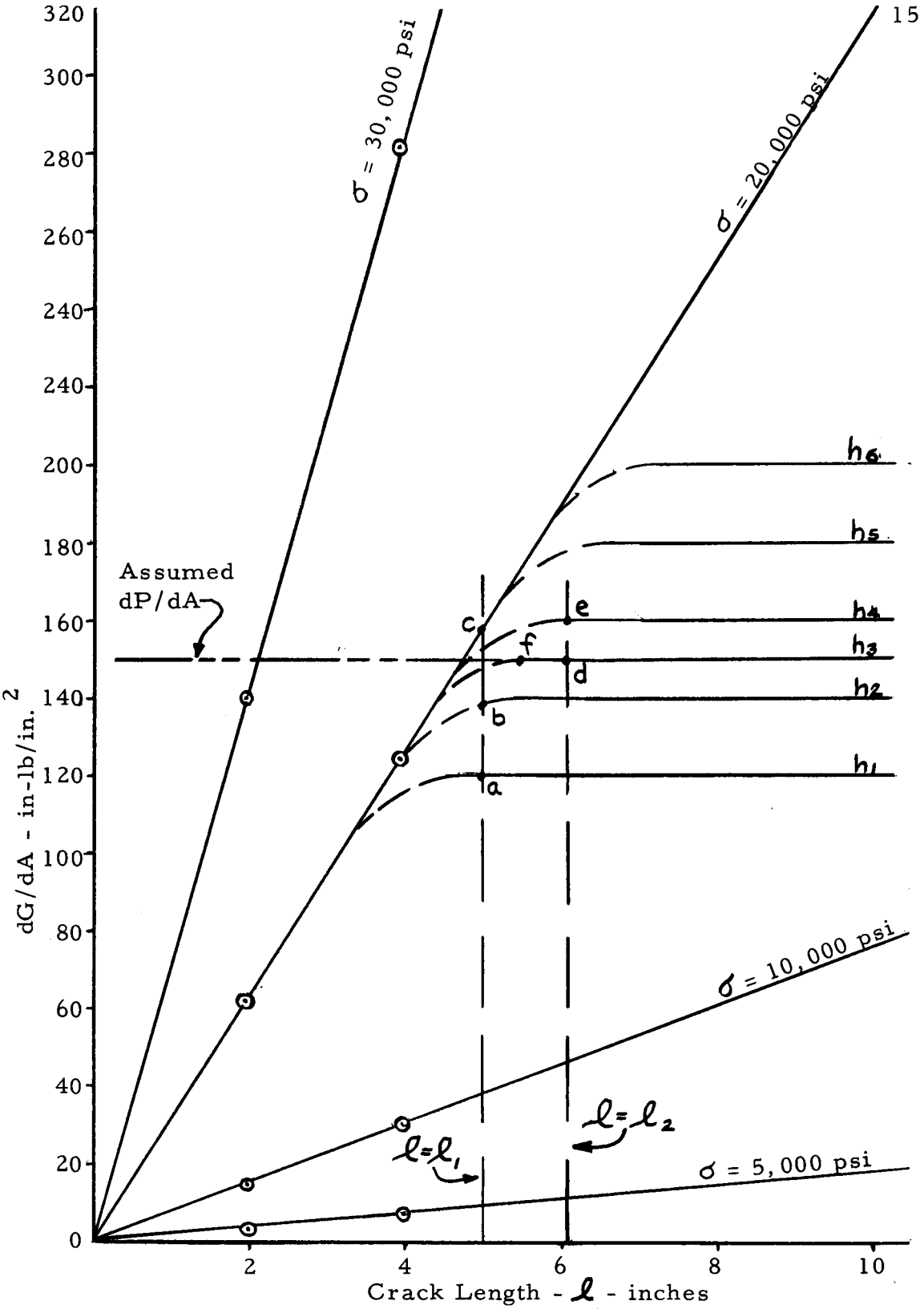

Fig. 4. dG/dA Calculated for Values of Crack Length.

is still applicable,

$$\frac{dP}{dA} = \frac{dG}{dA}$$

it can be seen that as h/2 increases some value will be reached at which instability occurs. Hence, a horizontal line can be drawn on the graph which corresponds to the critical value of dG/dA.

Between the region of $h/2 = \infty$ and h/2 much less than "b", there is a transition region in which both ℓ and h have some effect on the tendency for instability. Since no reliable theory has yet been established for this transition region it is impossible to predict the exact shape of the curve in this region. It is probable, however, that the transition will be a smooth curve as shown in Figure 4.

The significance of these curves can be illustrated by two examples. Consider two cracks of lengths ℓ_1 and ℓ_2 for a given value of stress. The conditions for instability are then determined by the values of h.

For $\ell = \ell_1$ and $h=h_1$ the value of dG/dA is given by point "a" and is less than dP/dA, therefore, the crack is stable. For $h=h_2$ the value of dG/dA is in the transition region shown by point "b" but since dG/dA is less than dP/dA the crack should still be stable. At $h=h_4$ the value of dG/dA is given by point "c". In this case dG/dA>dP/dA and the crack will be unstable. The value of h does not affect the stability in this case.

For $\ell = \ell_2$ and $h=h_3$, $dG/dA = dP/dA$ and conditions are critical, and for $h=h_4$, $dG/dA > dP/dA$ and the crack is unstable. It is important to realize that the value of ℓ is not of controlling importance as far as instability is concerned for these latter cases. The value of ℓ_2 may decrease to the point indicated by f before the entrance into the transition region begins to cause changes in ℓ to have an effect on dG/dA. The only variable which determines instability in the last two cases discussed above is the boundary spacing h.

The preceeding discussion of theory was for the case of a rapidly propagating crack. It has been found, however, that a crack has more than one mode of propagation through a ductile material. In discussing crack initiation and propagation it is convenient to divide the fracture process into three parts: crack initiation, slow crack extension, and fast crack extension to failure. In most materials the process of crack initiation usually involves a stress concentration which occurs in association with a geometric discontinuity. These discontinuities are the result of flaws in the materials, holes and joints in the structure, fatigue cracks, and fabrication defects.

The characteristics of slow crack propagation are also dependent on several different factors and particularly on the type and rate of loading. There are three phenomena which will cause slow crack extension: (1) local variations in the materials properties induced by loads that continuously increase over a limited period of

time, as in a tensile test, (2) local failure in the material wrought by a steady load applied over a long period in the presence of high temperature or adverse atmosphere, and (3) local changes induced in the material by repeated loads. The first of these cases is of the most interest since it is involved in the current series of tests. Investigations of slow crack extension under these loading conditions have shown that the farther the slow crack extends prior to complete fracture, the lower the load that is needed to cause instability and a runaway condition. It has been shown that this inverse function is the product of the stress at fracture times the size of the crack surface area due to slow crack extension and is equal to a constant. Or:

$$\sigma_f A = C$$

It has been further shown that this constant is G the amount of energy that must be added to open the crack to the critical point of instability (6, p. 30).

There is, however, one other factor which must be taken into account in the discussion of this process. This is the hypothesis that as the crack progresses, the size of the zone of plastically deformed material at the tip of the crack increases which in turn increases the resistance of the material to crack extension. However, as the amount of crack extension per unit stress increment increases due to an increase in the overall stress the process eventually ceases to be self-limiting so that the crack extends without any further increases

in stress. Figure 5 shows the relation of the stress on the material to the crack length. As the stress is increased the crack will progress from the steady state to slow crack growth to rapid crack growth and fracture as the length of the crack is increased (3, p. 389).

Some factors which may affect the process of slow crack extension are: material properties, section size, temperature, environment, and loading history. Irwin has correlated the effects of stress on the tendency towards slow crack growth and has expressed this relation in terms of a stress-intensity factor, K. As the stress increases and the crack length increases, the value of the stress intensity factor will also increase until it reaches a value of K_{I_c} at which point the crack will begin to propagate slowly. As the stress continues to increase to its maximum value the value of K will also increase until it reaches a value of K_c at the maximum value of stress and at which time the crack will propagate catastrophically (3, p. 390).

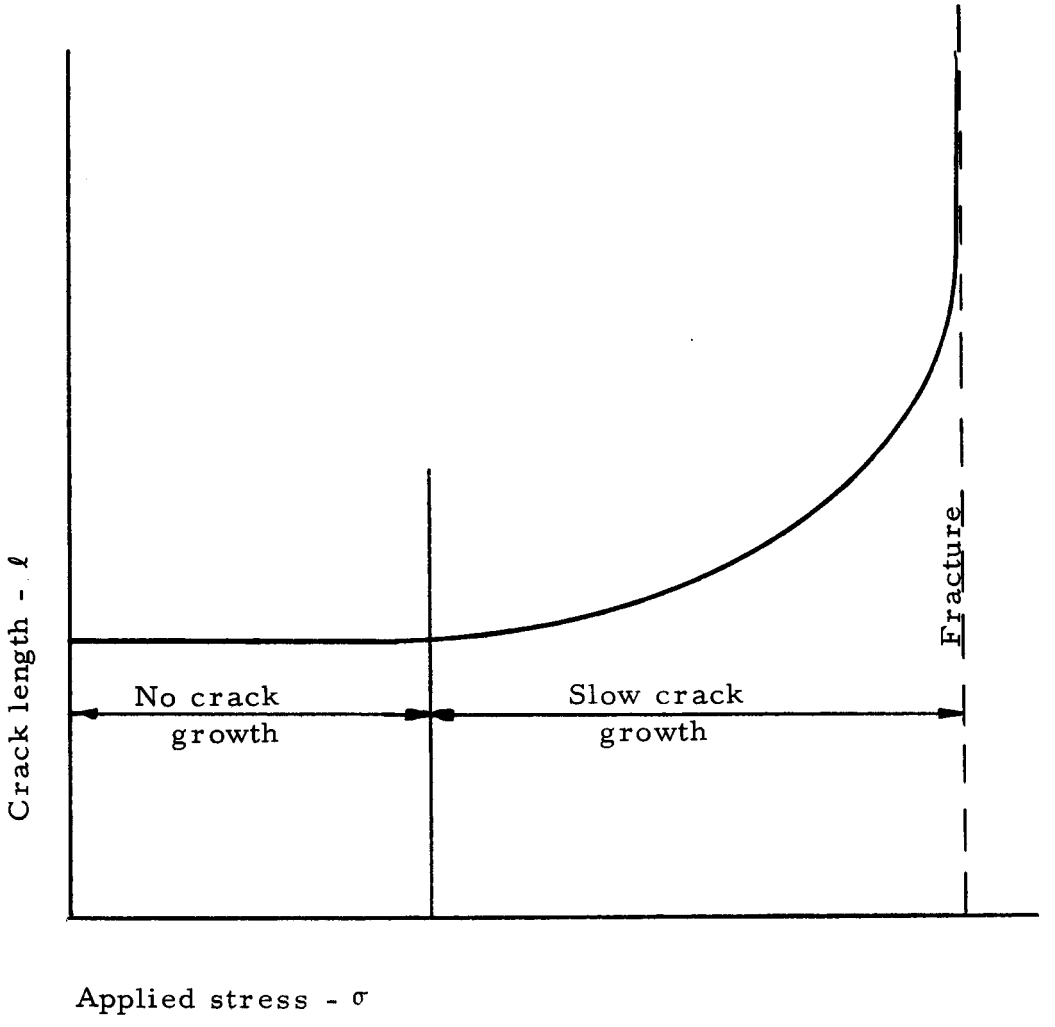

Fig. 5. Qualitative Relation Between Stress and Crack Length Showing Various Stages of Crack Growth.

EXPERIMENTAL STUDIES
PHASE ONE

Experimental Equipment

The design of the experimental equipment involved consideration of the various assumptions that were made in deriving the theoretical basis for the tests that were to be performed. However, since there was no method available for definitely determining the magnitudes of several of the variables involved it was necessary to design the apparatus in such a manner that tests could be run under a wide range of testing conditions. Since it was anticipated that changes would have to be made in the basic test setup, the equipment was constructed out of wood in order to facilitate these changes when they became necessary.

The test frame was constructed from two by four inch fir lumber and was bolted together in order to allow it to be dismantled and moved. The finished frame is shown in Figure 6. In order to simplify the specimen loading operation the foil sheets were tested by mounting them vertically and using dead weight loading. The supporting frame was built to sit on a table and allow the foil and weights to hang over the edge.

The foil sheets were attached to the supporting frame through clamps which gripped the foil during the test. These grips were

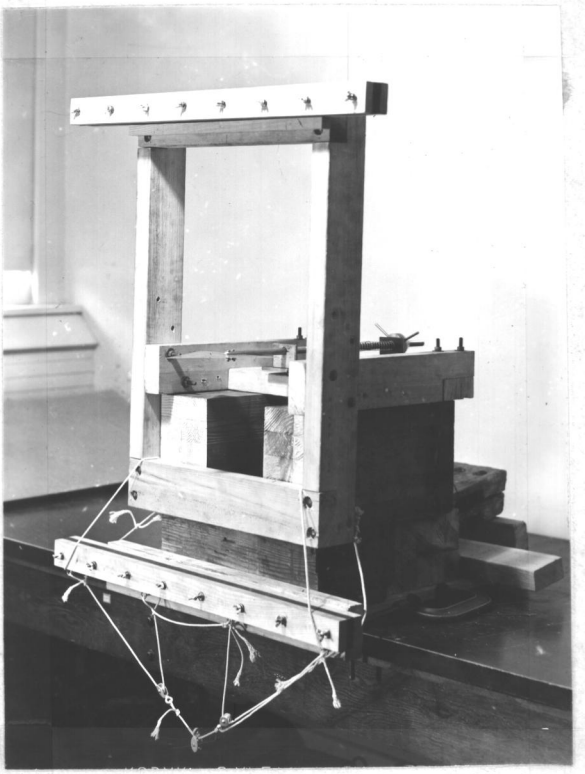

Fig. 6. Testing Apparatus for Phase One.

constructed out of ash hardwood and were made long enough to allow for testing under a wide range of geometrical configurations. A photograph of the finished clamps is shown in Figure 7. The interior surfaces of the clamps were lined with strips of foam rubber weather stripping to assure an even distribution of the load along the edge of the foil and to assure a secure grip on the foil so that it would not tear or pull loose from the clamps when the stressing load was applied. The foil was secured in the clamps with eight machine screws and wing nuts on each clamp. The upper clamp was fastened directly to the supporting frame and the lower clamp was allowed to hang freely from the bottom edge of the foil. Screw eyes were inserted into the lower clamp and nylon cord was attached with which the load was applied through a system of pulleys which evenly distributed the load along the length of the clamp. The load consisted of a series of lead weights which were suspended in a steel sling attached to the harness on the lower clamp. In some of the tests the loading weights were only used during the initial stressing of the material. Once the load was applied, the lower clamp was fastened securely to the test frame for the duration of the test. This procedure was necessary in order to justify the assumptions of a constant load on the material and no work done on the system during fracture, which were made during the development of the theory.

The cracks in the stressed foils were initiated through the use

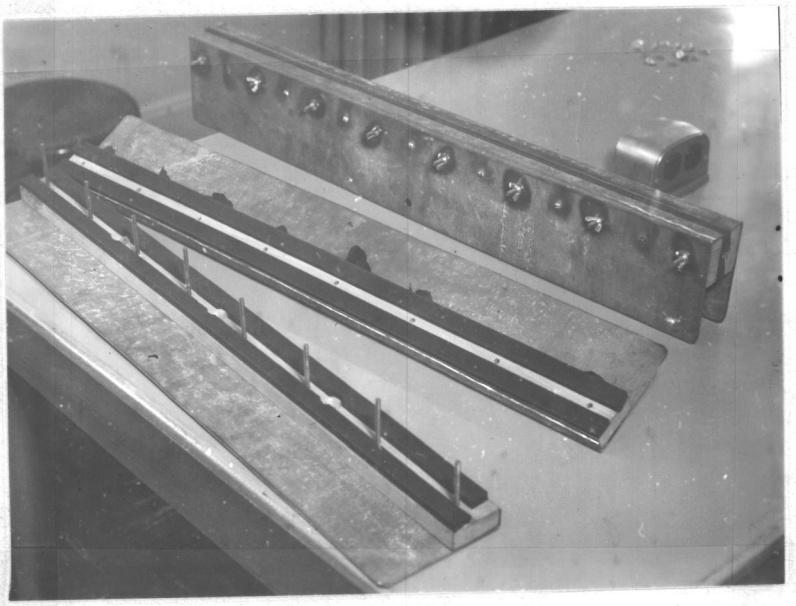

Fig. 7. Foil Clamps.

(Note foam rubber lining on disassembled clamp.)

of a triangular shaped knife blade which was moved through the foil. This allowed the crack to be initiated at the center of the foil and propagated outward an equal amount in each direction. This was accomplished by mounting the knife on the end of a long threaded rod. The rod was mounted in a bracket and was moved through the foil by turning a large micrometer nut which was placed on the rod. The knife blade mechanism is shown in Figure 8. Springs were added to the rod to assure that all the slack would be eliminated. The knife blade was prohibited from turning by a small foot attached to the rod which ran in a track milled into the base plate. A scale was provided on the base plate so that the travel of the knife could be measured and calibration marks were placed on the large turning nut so that it could be used as a micrometer. Since the rod was threaded with twenty threads to the inch, and the micrometer nut was divided into ten divisions, this provided a reproducibility of knife movement of 0.01 inches. The angle on the point of the knife blade mechanism was cut to 62.0 degrees in order to simplify the calculation of the crack length from the micrometer readings and the knife blade angle since the tangent of 62° is 0.600.

The knife blade mechanism was mounted on the support frame so that there would be a maximum possible travel of the blade of about five and one-half inches. The cutting blade was made from a sheet of thin steel which was sheared to size and the cutting edges ground and

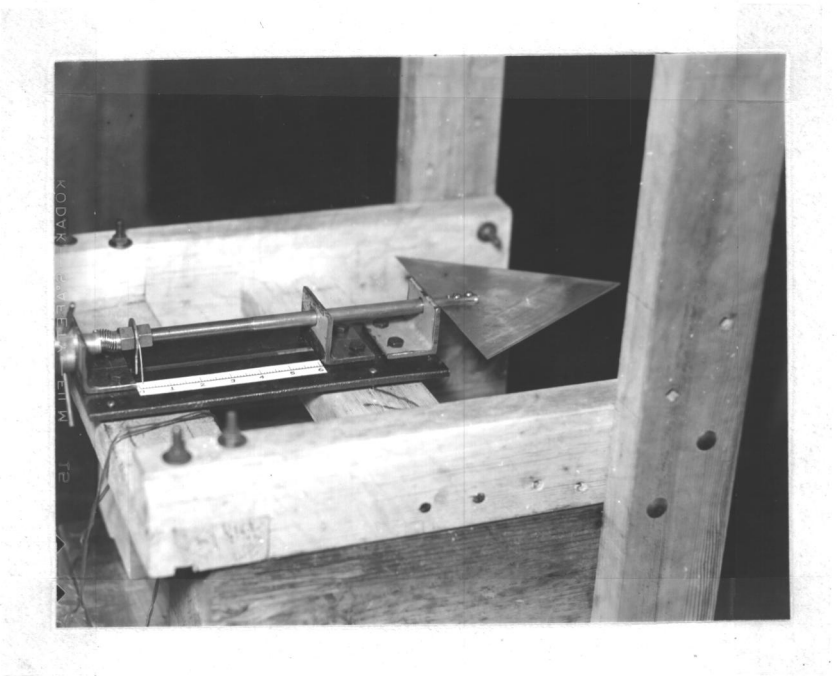

Fig. 8. Knife Blade Mechanism.

honed until a very sharp edge was obtained. It was necessary to grind a long taper on the blade so that the thicker part of the blade would not affect the cutting action of the edge.

Experimental Procedure

The testing program in which the wooden testing frame was used represented the initial efforts to correlate experimental work with theory. In these tests the foil sheets, which were made from household aluminum foil and which measured approximately 32 by 18 inches and were 0.001 inches thick, were mounted in the end clamps using two spacer sheets of masonite which were to insure that the foil was placed in the clamps squarely. First, the top edge of the foil was mounted in the upper clamp and then the lower clamp was attached to the bottom edge of the foil. The sheets of masonite were then removed and the aluminum foil checked to see that there was no wrinkling or tearing in the edges. The clamps were also checked to be sure that they were parallel to each other. If the foil was then found to be satisfactorily mounted the dead weight loads were applied by lifting the lead weights up and hooking them onto the nylon harness which was attached to the lower edge of the bottom clamp. The weights were then lowered until the full load was supported by the foil.

Providing that fracture did not take place during this phase of the operation, due to excentric loading or small tears in the edges of

the foil, the crack was then initiated in the foil. This was accomplished by rotating the micrometer nut on the knife blade mechanism in such a manner as to cause the knife to pierce the foil and form a crack of increasing length as the knife continued to move. This procedure was continued until the crack began to run under the action of the applied loads and ended in failure of the material. The crack length was then noted in order to calculate the energies involved. In some of the tests in this series the lower clamp was fixed to the body of the test frame by using "C" clamps which resulted in the load theoretically being held constant and no work being performed on the boundaries.

Experimental Results

The results of the tests were inconclusive. Catastrophic crack propagation appeared to occur during some of the tests but there was no reproducibility from one test to the next. The tests which did show this phenomenon were run with the boundaries free so that work was done on the system. Rapid crack extension was not observed, however, in the tests where the lower boundary was clamped. Several of the other tests in this series ended in premature failure because of tearing of the foil caused by non-uniform stressing of the foil or slippage in the foil clamps. Also, in all of the tests in this phase the strain relieved area was observed to intersect the boundary clamps

thus making the assumed theory inapplicable.

Analysis of Experimental Equipment

Obviously, this equipment did not operate properly under all of the previously mentioned conditions. The basic design was satisfactory in principle but there were certain disadvantages in the operation. The greatest problem which occurred involved the load application system. In order to create a stress of high enough magnitude to cause catastrophic crack propagation it was necessary to use loads approaching 200 pounds. This was accomplished by using 50 pound slabs of lead which were piled on the loading sling attached to the lower foil clamp. However, it became difficult to apply the load evenly so as to avoid impact loading and to avoid causing eccentric loads on the foil. The best method seemed to be to place all the weights in the sling and then lift then into place on the clamp. The main difficulty was encountered in lifting the 200 pound loads into place without jerking or tearing the foil.

Problems were also encountered in attaching the foil clamps to the test frame, so that the conditions of no work on the boundaries could be established, due to the lower foil clamp's position below the bottom of the supporting frame. It was also difficult to mount the foil in the clamps so that the clamps were always parallel and the foil was always vertical. For these reasons and the fact that it was not felt

that the wooden frame satisfied the requirements of a rigid structure under these loads it was decided that a different apparatus should be employed in which these problems would be alleviated.

EXPERIMENTAL STUDIES
PHASE TWO

Experimental Equipment

In order to alleviate the problems encountered in the first set of tests, the foil clamps were shifted to a vertical creep testing apparatus which was available at the time. The creep equipment was originally designed to test strands of wire under high stresses at elevated temperatures. It was therefore necessary to convert the machine to conform to the requirements of the present tests. The machine consisted basically of two vertical channels on top of which was placed a counterbalanced lever. One end of the lever, which was mounted on knife edges, was fitted with an adaptor which attached to the creep specimens. The other end was used for applying the load. The lower grip for the creep specimens was attached to a large, square thread screw mounted on the machine with which the load was applied.

The conversion process consisted of removing the furnace from the apparatus and adapting the creep grips so that they could be attached to the foil grips. The knife blade mechanism was also removed from the original apparatus and mounted between the two pieces of supporting channel flanges. In order to facilitate the mounting of the foil in the grips and also to increase the rigidity of the grips,

pieces of sheet metal were clad to the clamps using wood screws with holes drilled to make clearance for the clamp tightening screws.

Figure 9 shows the apparatus after the conversion had been completed. The loading lever had a ten-to-one ratio so that to have a 150 pound load on the foil it was only necessary to add 15 pounds to the rear of the lever. Attached to the front end of the loading lever was a second knife edge from which was suspended a ball swivel joint on which the upper foil clamp was hung. The swivel joint allowed the clamps freedom of movement in all planes and assured that there would be no eccentric loads applied to the foil.

Experimental Procedure

The second series of the experimental tests using the modified creep testing machine were similar in procedure to the first series of tests except that the mechanical features of the equipment allowed a higher degree of accuracy to be attained while more careful observation of the crack could be made than was possible with the original equipment. The operation of this equipment consisted of mounting the foil in the same set of clamps that were used in the original tests although, as previously mentioned, the clamps were not rigidly fixed to the body of the machine. The foil was laid out on a table and the clamps were attached to each end. The squareness of the clamps was insured by measuring the foil instead of using the masonite sheets.

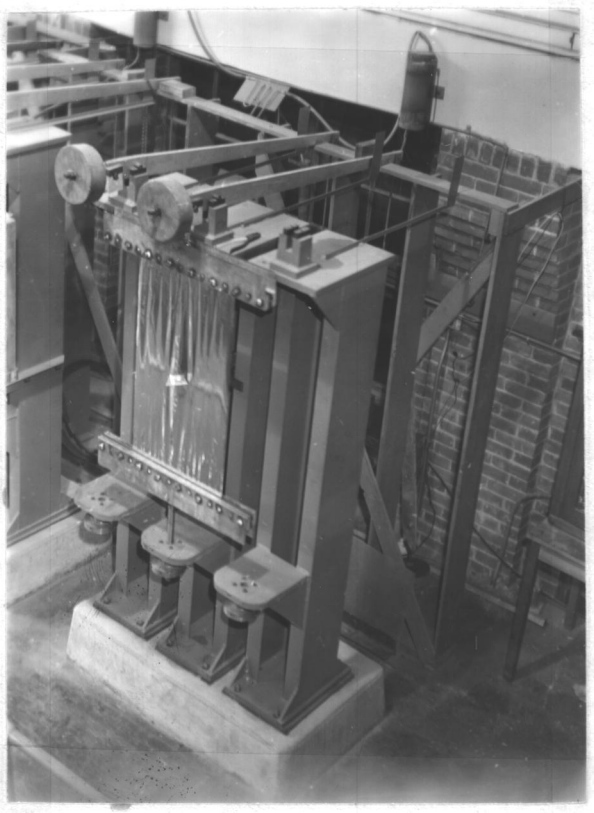

Fig. 9. Test Apparatus for Phase Two Using Converted Creep Tester.

The clamps were tightened and the complete assembly lifted into place on the machine. With a small amount of practice this could be accomplished without any wrinkling of the foil. The upper clamp was hung on the swivel joint attached to the loading lever and the bottom clamp was attached to the jack screw. The desired load was then placed on the rear end of the loading lever and the screw was tightened until the lever was lifted from its support. At this point the desired stress was present in the foil and the crack was then initiated in the foil using the knife blade mechanism and the same methods as were used in the first series of tests.

The running of an actual test involved the manipulation of several different parts of the machine and the observation of different phenomena at the same time. This led to operational difficulties due to the fact that the construction of the basic testing frame prevented the operator from being able to reach both the load application screw and the micrometer nut on the knife blade mechanism simulataneously. This was the result of using previously constructed equipment which was not precisely suited to this application. The micrometer nut was located behind the testing frame and close observation of the progression of the crack was not possible although it was not completely unobservable. The inaccessability of the loading screw made it difficult to apply the load but the problem was overcome by loading the foil to a point such that the loading lever was lifted high enough

from its supporting blocks to accomodate any drop that might occur during the test due to the elongation of the sheet. This, of course, meant that work was done on the system and also that the stress was constantly increasing as the crack elongated due to a decrease in the cross-sectional area of the material. This made the determination of the stress that was present at the instant of criticality impossible since the crack length at criticality could not be determined.

In order to eliminate the work done on the system it was decided to place a block under the loading lever after the proper load had been applied. Once the lever was in the floating position, a small block was placed underneath the lever so that any downward movement of the weighted end of the lever was eliminated but no load was relieved from the lever initially.

Experimental Results

It was during the test runs under the latter conditions that the difficulties in crack length determination became apparent. It was noted that once the crack had been initiated and enlarged with the knife blade, the crack would jump ahead of the edge of the knife as though catastrophic propagation had begun except that it would fail to continue to grow and would stop. This would result in a decrease in the load due to the loading lever coming in contact with the supporting block which in turn would decrease the stress. However, once the

load was increased again the crack would continue to grow but would again stop for the reasons previously stated. This process would continue until a point was reached where the crack would continue to grow slowly and then would suddenly begin to propagate catastrophically.

Analysis of Experimental Equipment

It was obvious that catastrophic failure was occurring but it was impossible to exactly state the instant at which spontaneous propagation began and to specify the conditions under which it took place. Probably the hardest of the parameters to determine was the critical crack length. Since the crack would, in general, grow ahead of the edge of the knife blade it was not possible to use the micrometer readings as an indication of the crack length. Irwin (6, p. 36) notes experiencing the same problem and solved it through the use of ink staining in which a drop of ink was placed at the tip of the crack. The surface tension of the ink would allow it to follow the crack during slow crack extension but it would fail to keep up with the tip during rapid crack growth. Consequently, the point of criticality could be determined by noting the positions of the ink stains on the material adjacent to the crack. This method was not attempted, however, since the investigation became pointed towards the study of the effects of plastic deformation at the crack tip.

Since the occurrence of slow crack growth was obviously a contributing factor in the fracture process which affected the critical length and the stress conditions at the instant of catastrophic failure it was desirable to investigate the conditions of slow crack growth so that the phenomenon of rapid crack growth might be better understood.

EXPERIMENTAL STUDIES
PHASE THREE

Investigation of the available literature on slow crack growth showed that one important assumption involved the existance of an area of plastic deformation preceeding the tip of the crack whose size continued to increase as the crack progressed (10, p. 8). If this was true it appeared to be of major importance and it was decided to study the plastic deformation that preceded the tip of the crack as it progressed.

Experimental Equipment

In order to obtain a visual observation of this phenomenon, small specimens of foil were mounted in a drill press vice with which the foil could be stressed. A small crack was introduced into the center of the foil and parallel to the vice jaws by slitting with a razor blade. The vice was then inverted on the stage of a metallograph and a series of photomicrographs were taken at various positions of the crack as it progressed due to increases in the distance between the vice jaws. These photomicrographs are shown in Figure 15.

A series of tests were also run in which the amount of deformation occurring in the material as the crack progressed was actually measured. This was done on a Tukon microhardness tester which was adapted for use under the particular conditions of these

tests. The microhardness tester consists of an indentor, an indentor loading system, and an identation measuring microscope. The specimen and the vice are mounted on a microton which is movable in two dimensions so that the specimen may be positioned under the indentor. The microton is mounted on a slide which allows a particular part of the specimen to be positioned under the indentor and then slid forward so that it comes directly under the microscope. Figure 10 shows a close up of the specimen and the microton.

Experimental Procedures

The specimens in these tests were sheets of foil about one and one-half inches wide and three inches long which were mounted in a drill press vice. This allowed the foil to be stressed by turning the screw on the vice. See Figure 10. The indentations on the foil were made by placing a polished piece of copper behind the foil to give it support and using the lightest available load on the indentor. These indentations were later used for measurement purposes. The actual indentation process was automatic once the specimen had been positioned under the indentor and the result was a diamond shaped impression on the surface of the foil. The points of the diamonds were used for measuring the distances between the various impressions and for determining the amount of deformation which occurred during stressing. The microscope was equipped with a scale and a

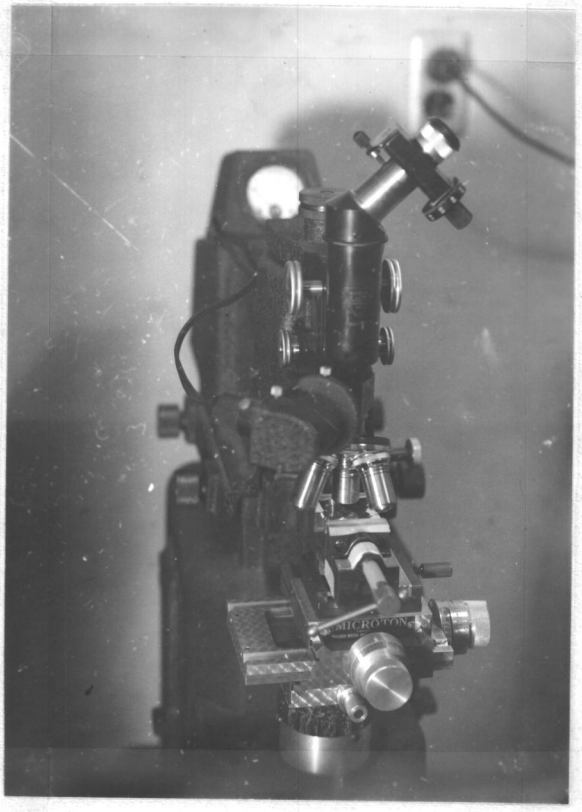

Fig. 10. Microton and Specimen on Microhardness Tester Used in Phase Three.

movable hairline so that the distances could be read from the scale without moving the specimen. The micrometer screws on the base of the microton were used in the determination of the distances from the tip of the crack to the various sets of indentations. The unit markings on the screws were equal to 0.01 millimeters. Figure 11 shows a typical crack tip and indentations.

A small crack was introduced into the center of the sheet with a razor blade and each end of the crack was given a sharp tip. The vice was then mounted on the microton of the microhardness tester and the impressions were placed on the foil. In the first set of tests, six indentations were made perpendicular to the axis of the crack and approximately five-eighths of an inch ahead of the tip. The initial distance from the tip of the crack to the set of indentations was accurately measured along with the distance between the indentations. The vice screw was then turned a small amount and the distance between successive pairs of indentations and the distance to the crack tip was again measured. This process was continued until the crack had progressed past the position of the indentations on the foil. The differences in the distances were calculated and the results used as a measure of the amount of deformation of the foil for each increment of crack elongation. These values of deformation were then plotted versus the crack tip to indentation distance as shown in Figure 16. The results of this graphical presentation are discussed in a later

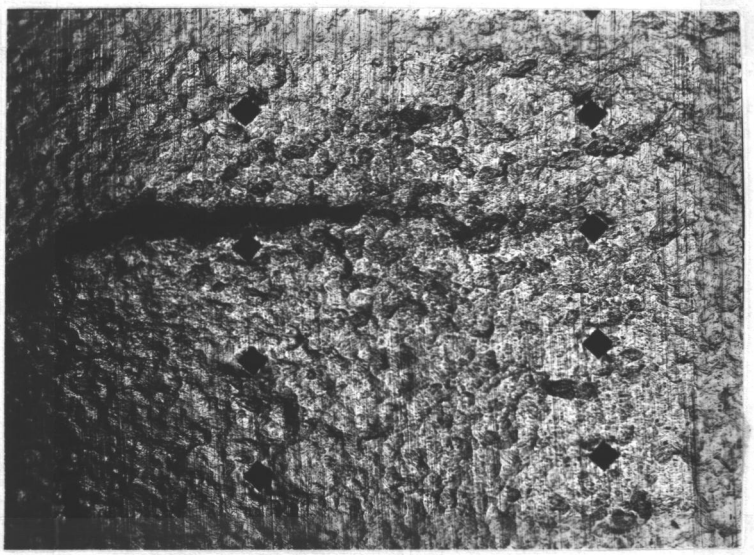

Fig. 11. Typical Crack Tip and Indentations.

section.

In order to determine whether there were any transient effects present during the first series of tests a second type of test was run to check the results of the first tests. The second tests were similar to the first ones except that a larger number of indentations were used. Eleven sets of eight indentations each were laid out on the foil perpendicular to the axis of the crack. The arrangement is shown in Figure 12. This arrangement allowed the distribution of strain in the plastically deformed region to be fully determined for varying positions of the crack and made it possible to determine the changes in the plastically deformed region as the crack progressed from its initial positions to its final position past the last set of indentations. The data were taken in the same manner as in the first series of tests. The total elongations of each set of indentations have been calculated and are plotted in Figure 17. This method of analysis was chosen in this case in order to give a better overall picture of the variation of the strains in the material for different distances from the crack tip. Each curve represents a new position of the crack tip as shown by the arrows on the curves. These results will be discussed later.

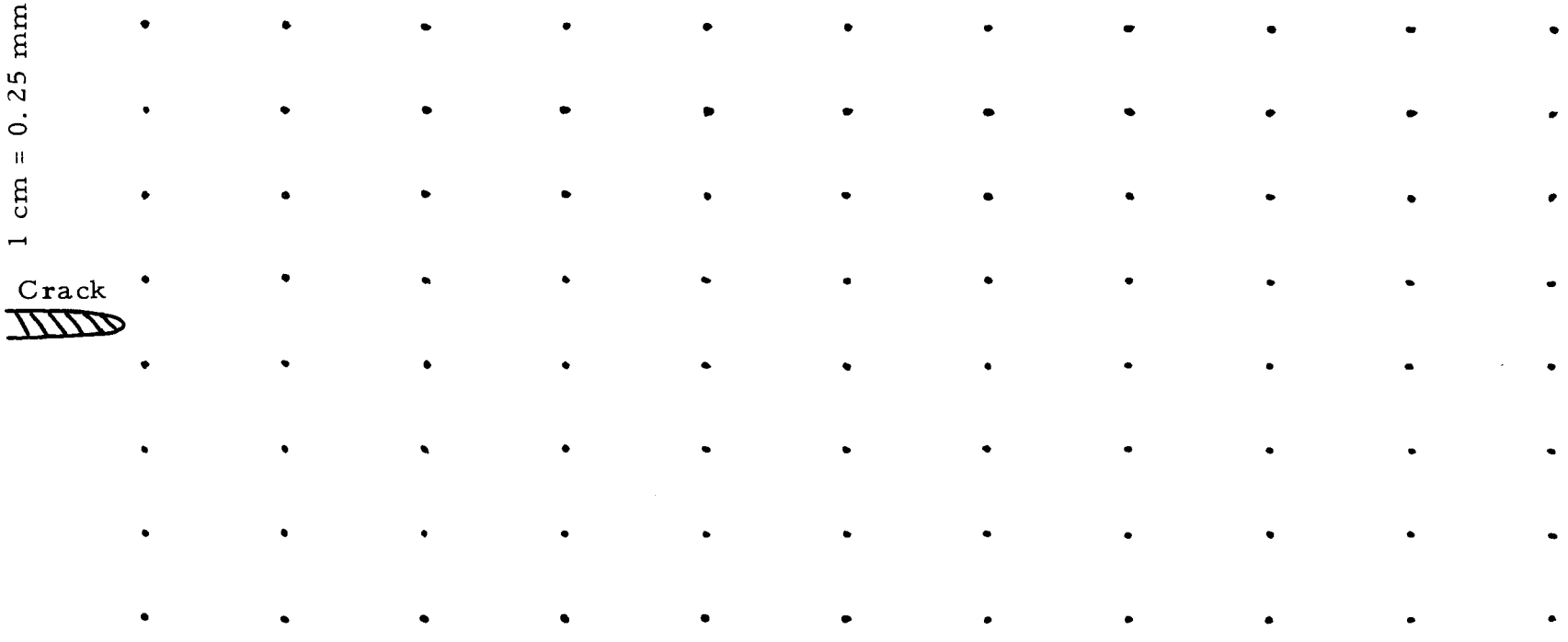

Fig. 12. Diagram of Indentation Positions on Foil Surface for Second Series of Deformation Tests.
1 cm = 0.5 mm

DISCUSSION

Many of the current mathematical and experimental investigations of the phenomena of crack growth are based on the determination of the amount of plastic and elastic deformation that occurs at the crack tip (10, p. 1). This determination is of particular importance when the characteristics of slow crack growth are being investigated. For example, it has been proposed that the starting and stopping action observed during slow crack growth is the result of an increase in the amount of plastic deformation that occurs in the material surrounding the tip of the crack (3, p. 389).

It has been commonly assumed for the sake of simplified mathematical analysis that the area of plastic deformation approximates a circle which is tangent to the crack tip and which extends into the uncracked material. This configuration is shown in Figure 13. It has been used in conjunction with an analysis of the case of shear loading of the crack. This model has been modified for the tensile case by assuming that the zone of plastic deformation is elongated into the shape of an ellipse. This configuration is shown in Figure 14 (10).

On the basis of visual observation, through the use of a metallograph, of the area of plastic deformation during crack growth it appeared that there was no definite boundary between the plastic

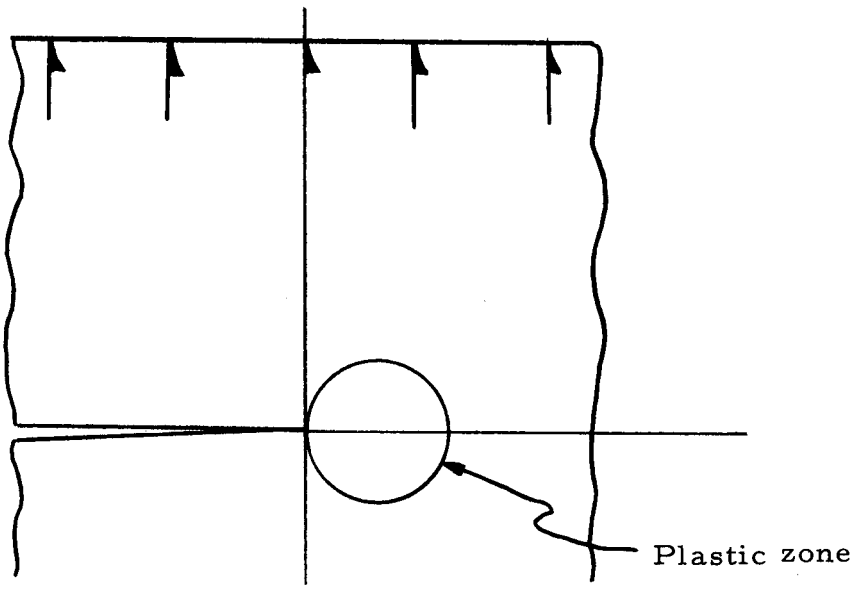

Fig. 13. Plastic zone for shear case.

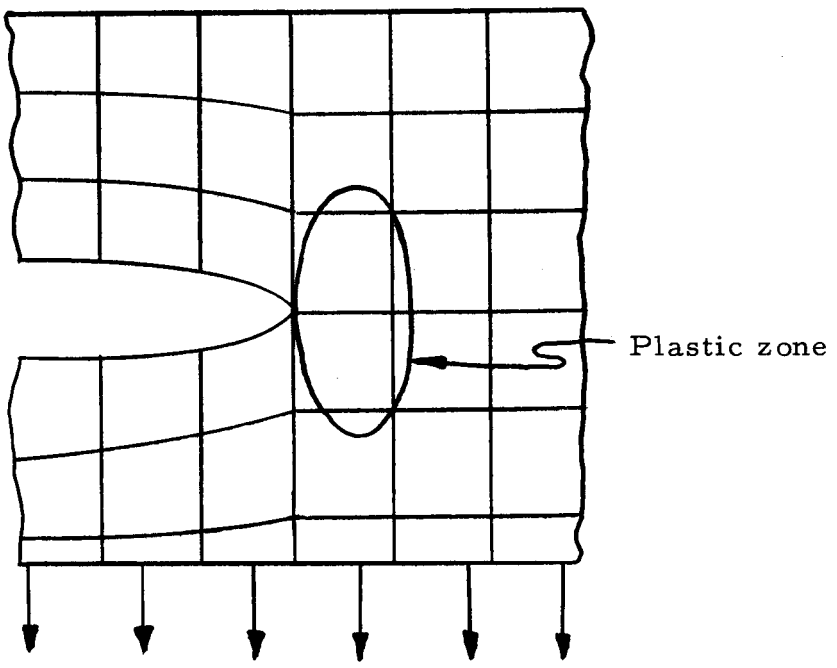

Fig. 14. Plastic zone for tensile case.

and elastic area. This conclusion is supported by the photomicrographs shown in Figure 15 which is a series of photographs which were taken at various stages of growth of a tensile crack. Figure 15 a shows the original crack as introduced by the razor blade. The dark parabolic area is due to the fact that when the crack was introduced into the foil there was a certain amount of bending of the foil adjacent to the crack and as a consequence the light from the illuminator of the metallograph was not reflected back into the objective and the area appears dark. The actual crack is located in the center of the dark area and approximately three-eighths of an inch back from the rounded point in the figure. The condition of the as-received foil may be observed here and it will be noticed that the crack was introduced perpendicular to the rolling direction as indicated by the rolling marks on the surface. The load was applied parallel to the rolling direction.

Figure 15b shows the material just ahead of the crack after a slight increase in the strain has occurred. The crack is still not visible as it is located in the dark parabolic region as before. It will be noticed that plastic deformation has begun and it is located primarily in the area immediately ahead of the crack tip. The plastic deformation may be identified by the characteristic wrinkling or dimpling which it causes in the surface of the material. In this figure the plastic zone is highly localized and the remaining material

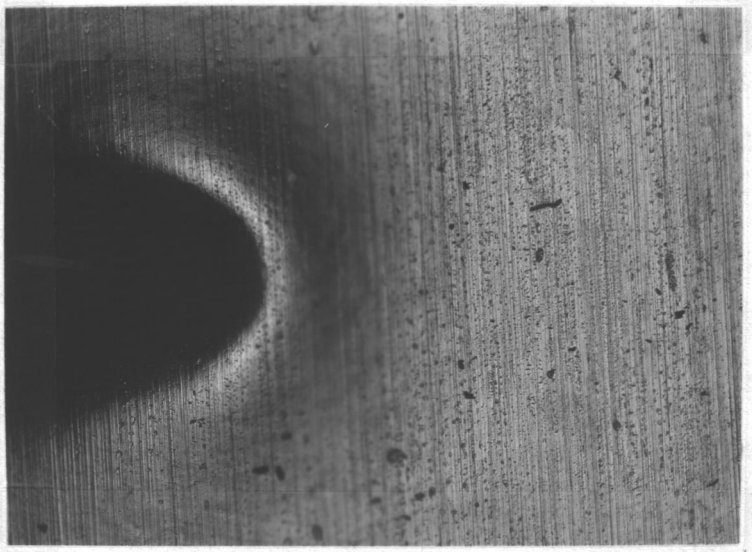

Fig. 15a. 47 x

Fig. 15b 47 x

Fig. 15. Photomicrographs of Foil at Various Stages of Crack Propagation.

is essentially unchanged. The relative positions of the crack in these photographs can be approximated by comparing the positions of observable markings on the surface of the foil.

Figure 15c shows the specimen after a further increase in stress. In this photograph the crack tip lies approximately at the edge of the darkened area. The area of the plastically deformed material is slightly increased and could even be imagined to roughly approximate an ellipse as has been previously discussed. It can be seen that there is a region of very intense plastic deformation directly ahead of the crack tip and the intensity of deformation decreases as the distance from the crack tip increases. This is to be expected although it is difficult to define a boundary between those areas of plastic deformation and the areas of elastic deformation. In fact, it was observed that small amounts of plastic strain occurred throughout the specimen and some can be seen in this figure at the right hand edge of the photograph.

In Figure 15d the stress has been further increased and it is possible to observe the crack projecting from the darkened area. The area of plastically deformed material continues to increase and it completely surrounds the crack tip. The amount of plastically deformed material in the rest of the photograph has also increased and further investigation of the extent of this plastically deformed area showed that it tended to extend throughout the entire specimen and

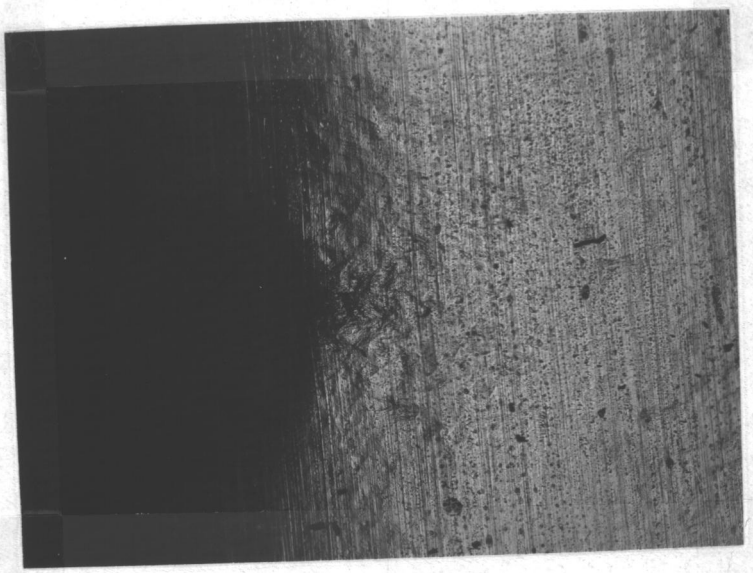

Fig. 15c 47 x

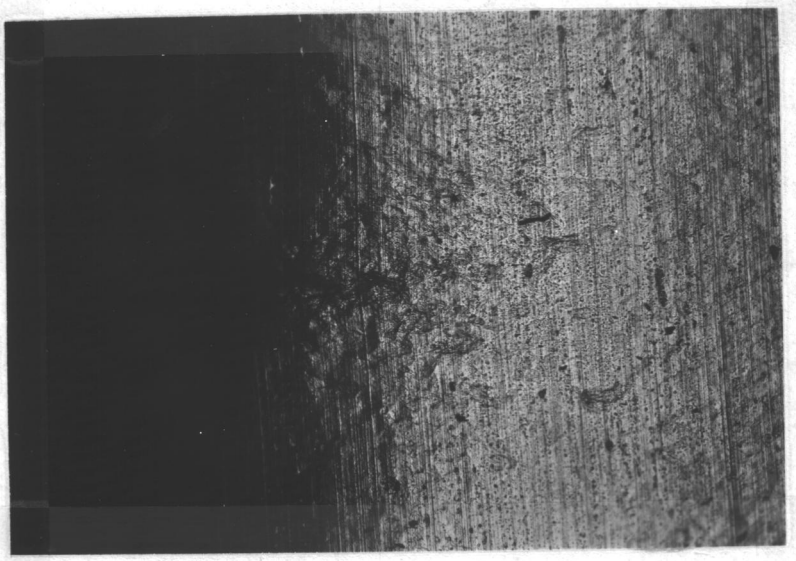

Fig. 15d 47 x

was not localized in one area around the crack tip.

Figure 15e shows the crack after further extension due to increased stress. It will again be noticed that a severe amount of plastic deformation surrounds the crack tip and the intensity of deformation decreases as one progresses out from the tip. At this point it is impossible to define any area at the crack tip which might be defined as containing all of the plastically deformed material. Instead, it is seen that plastic deformation has taken place throughout the material. The formation of small cracks ahead of the tip of the main crack is shown here and they may be identified by the intense amount of plastic deformation which accompanies them.

Figure 15f shows further progression of the crack with increased displacement of the vice jaws. Here again the severe deformation next to the tip is obvious and the decrease in deformation with increased distance away from the crack is apparent. Precracking is not as well observed in this photograph as in the previous one; however, the amount of plastic deformation in the rest of the material continues to increase.

Figures 15g and 15h were both taken after the crack had been further propagated a short distance. Figure 15h was taken with oblique lighting to emphasize the amount of plastically deformed material that was present. Figure 15g shows a good example of the formation of small cracks ahead of the actual crack tip. These small

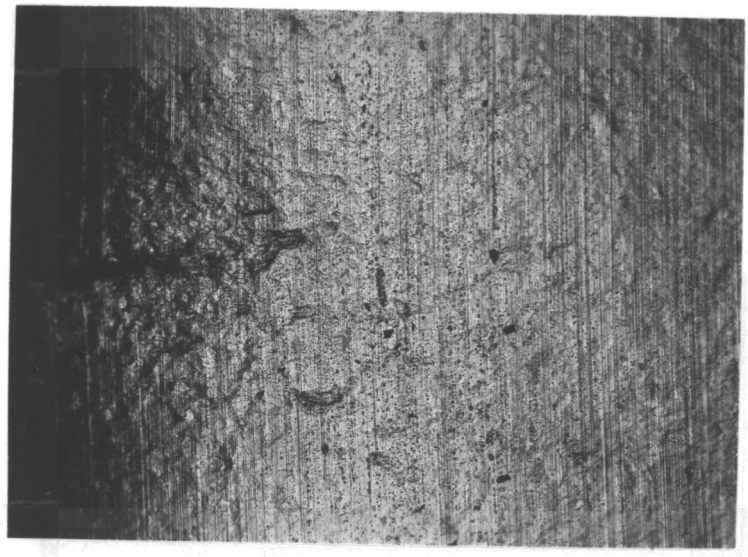

Fig. 15e 47 x

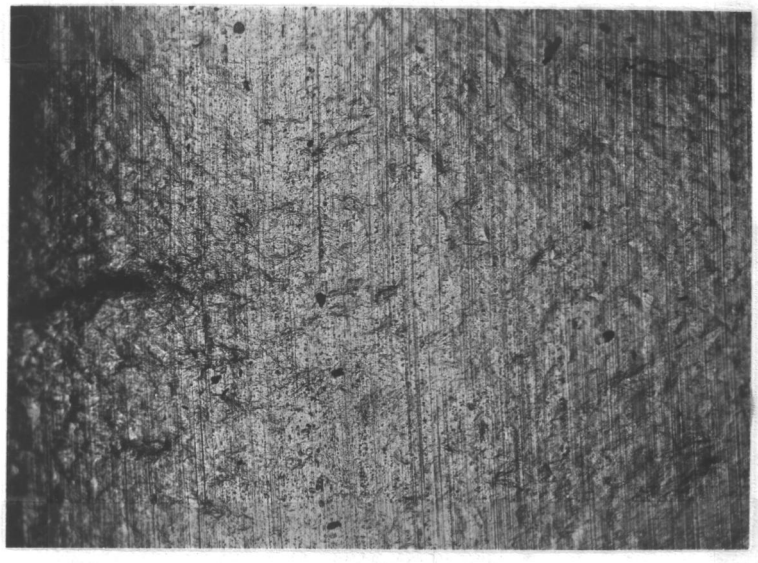

Fig. 15f 47 x

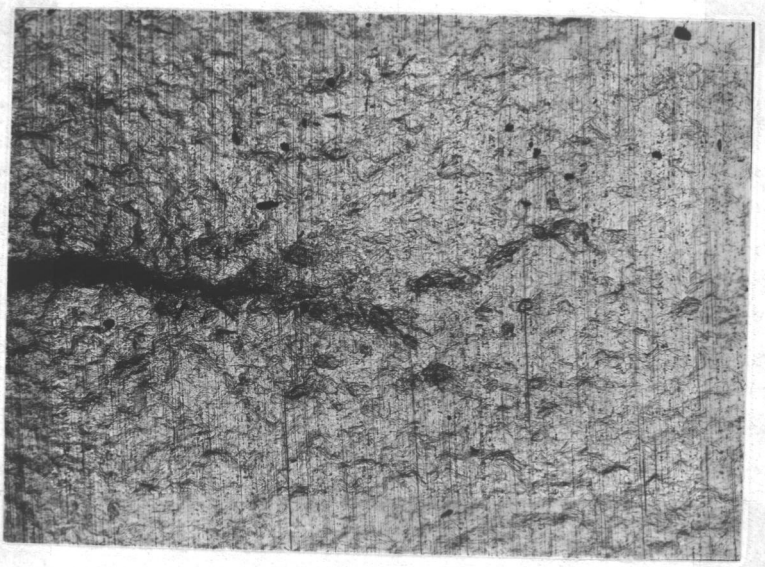

Fig. 15g 47 x

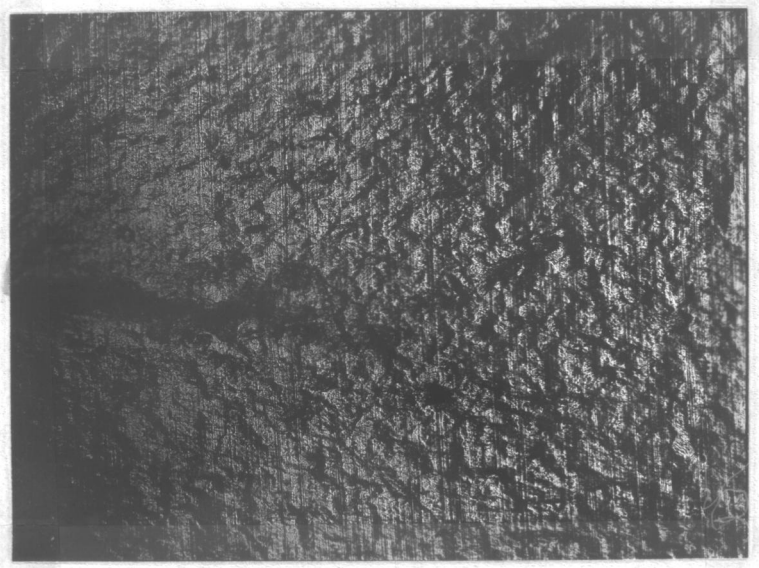

Fig. 15h 47 x

(Same as Figure 14g only with oblique lighting.)

cracks have an area of severe plastic deformation which surrounds them in addition to the deformation which is already present from the propagation of the main crack. These examples show very intense deformation around the crack tip and the deformation in the rest of the material appears to exist throughout. This is illustrated particularly well by the oblique lighting in Figure 15h. It was subsequently observed that the main crack joined the small crack which is beginning to form and continued to progress in that direction.

Figure 15i consists of two photographs which show the material ahead of the crack tip. It should be noted that the two parts of the figure do not exactly match at their adjacent boundaries but they are very close and they cover a distance of about 3. 3 millimeters ahead of the crack. The lower photomicrograph shows the material in the vicinity of the crack which is seen in the lower portion of the figure. Again, the severe deformation around the crack tip is shown along with the continued deformation of the material further away from the tip. The upper photograph was taken a short distance ahead of the crack and shows the amount of deformation which was present at a further distance than was shown in the previous photographs. The amount of plastic deformation is seen to decrease as the distance from the crack increases. At the top of the upper picture the amount of deformation has decreased to such a point that the surface nearly resembles the original material as shown in Figure 14a. Under

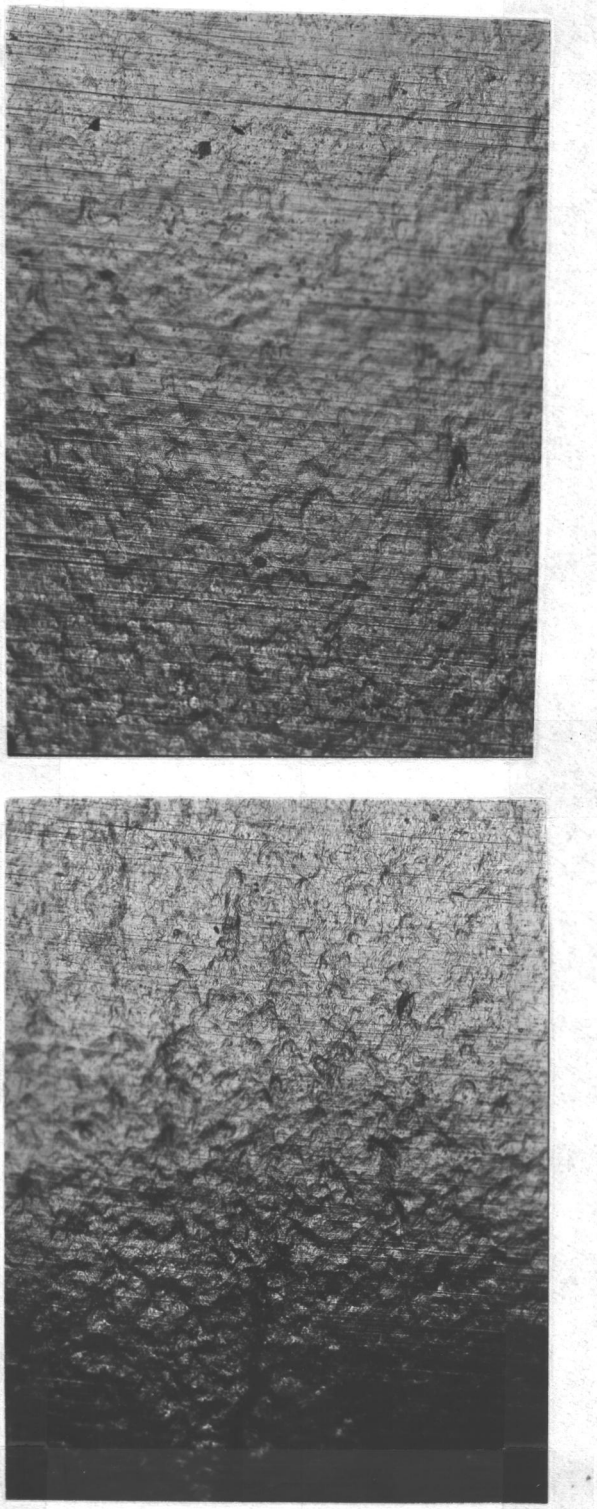

Fig. 15i 47 x

oblique lighting, however, some plastic deformation was still visible.

There are several observations which may be made in connection with the preceeding photomicrographs. The first and probably the most obvious is the fact that the zone of plastic deformation is not confined to an area which may be described by a simple geometrical configuration. As has been described, the plastic deformation appeared to extend throughout the whole volume of the specimen and it increased in intensity everywhere as the crack continued to grow. This would lead to the conclusion that there is an overall plastic strain which occurs in the material in addition to the local intense deformation which occurs as a result of the propagation of the crack tip. Therefore, it does not seem that the mathematical model of a definite zone of plastic deformation, with only elastic deformation occurring outside of the zone, is accurate.

The actual behavior for different materials will be variable. In the present set of tests the aluminum foil was very ductile. It is reasonable to assume that the amount of deformation in a less ductile material will be smaller, but it would not follow that even in such cases there would be a definite transition between the plastic and elastic conditions. More accurate analysis of the energy requirements for catastrophic propagation would necessarily involve a more complicated model in which the plastic deformation which occurs outside the regions of the previously assumed zone of plastic

deformation is taken into account, since it appears that the deformation in these areas is appreciable.

The results of the first series of tests in which the amount of plastic deformation was actually measured using the Tukon microhardness tester are shown in Figure 16. The individual curves are lettered A through E and they represent the spaces between the various indentations. The layout of the indentations is shown on the graph. Each curve shows the amount of deformation that was present in the material at the various stages of the crack growth. The two curves lettered A and E show the least amount of deformation while curves B and D exhibit somewhat more deformation. Curve C progresses vertically off the graph due to the crack having passed through this spacing Therefore, the distance between the spots on each side of this space was greatly increased.

It can be seen that the amount of deformation increases gradually as the position of the crack tip is approached. The crack tip may be considered to be located at zero on the abscissa. The deformation gradient becomes greater, however, as the crack comes nearer and in the region immediately in front of the crack there is a large increase in the strain. This coincides with the observations of the photomicrographs previously discussed in that there was a region of severe plastic deformation immediately ahead of the crack tip.

As the crack passes the position of the row of indentations, the

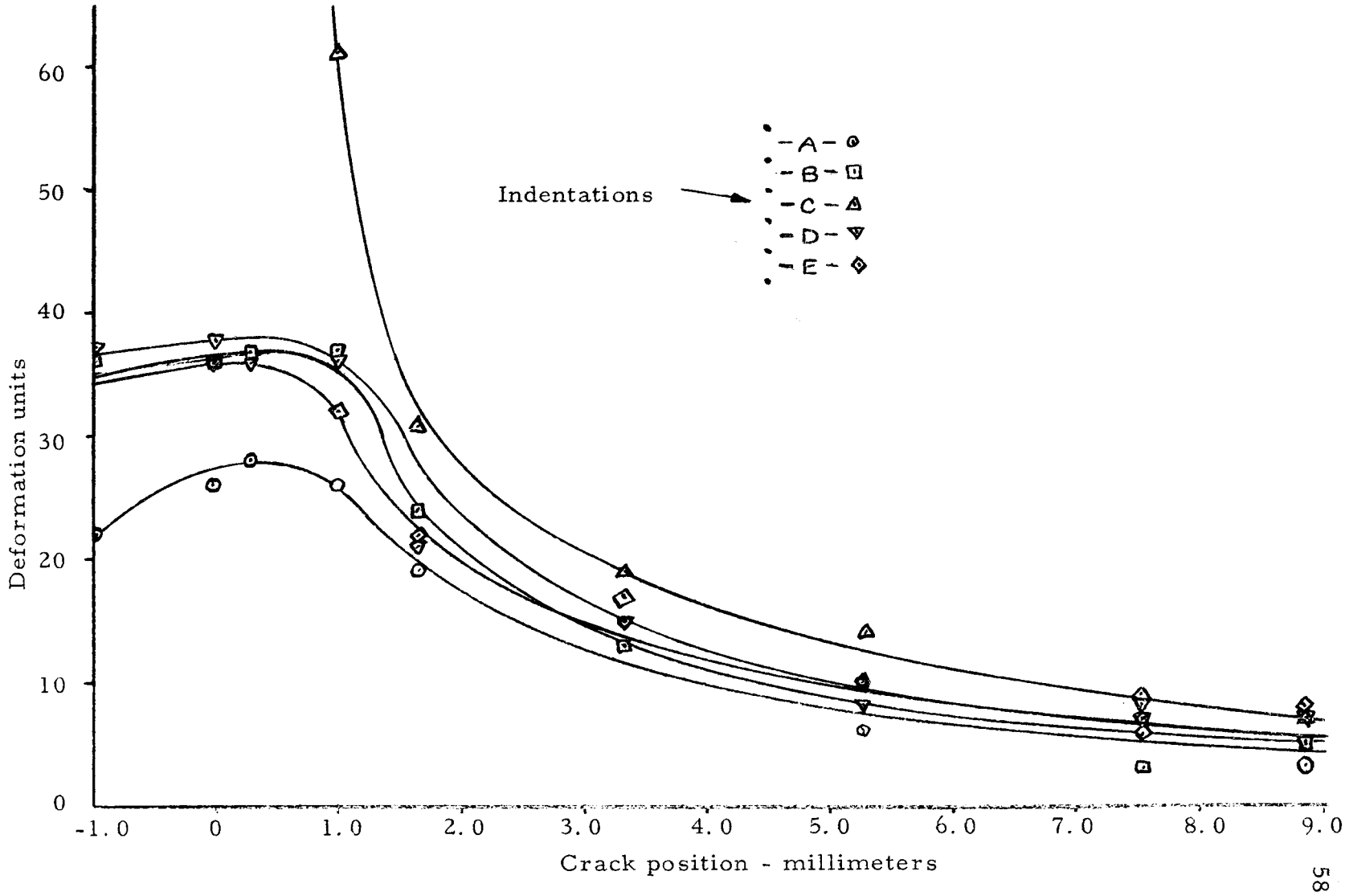

Fig. 16. Deformation of Foil with Variations in Crack Position.

strain gradient decreases and then becomes negative. This is due to the elastic recovery that takes place in the material when the stress is removed. The small decrease in the deformation curves occurring at the left hand edge of the graph, which corresponds to a position inside the strain relieved area, indicates that there is some elastic strain present in addition to the plastic strain in the stressed material ahead of the crack tip. The curve does not, however, indicate any point ahead of the crack at which plastic strain may be considered to begin. A number of specimens were tested in a similar manner using the single row of spots and all of the results were similar to those in Figure 16.

The results of the second series of tests which were run to check the transient effects of crack propagation are shown in Figure 17. Six curves are shown which represent six stages of the crack during its propagation and the position of the crack is indicated by the small arrow above each curve. The crack is propagating from left to right on the graph. Curve one shows the amount of deformation after the crack has been moved a small amount. It can be seen that there has been a general increase in the amount of strain as the tip of the crack is approached, but the strain gradient decreases rapidly as the distance from the crack tip is increased. Curve two is similar to curve one and shows further deformation in the material after the crack has been extended. There is a general increase in the amount

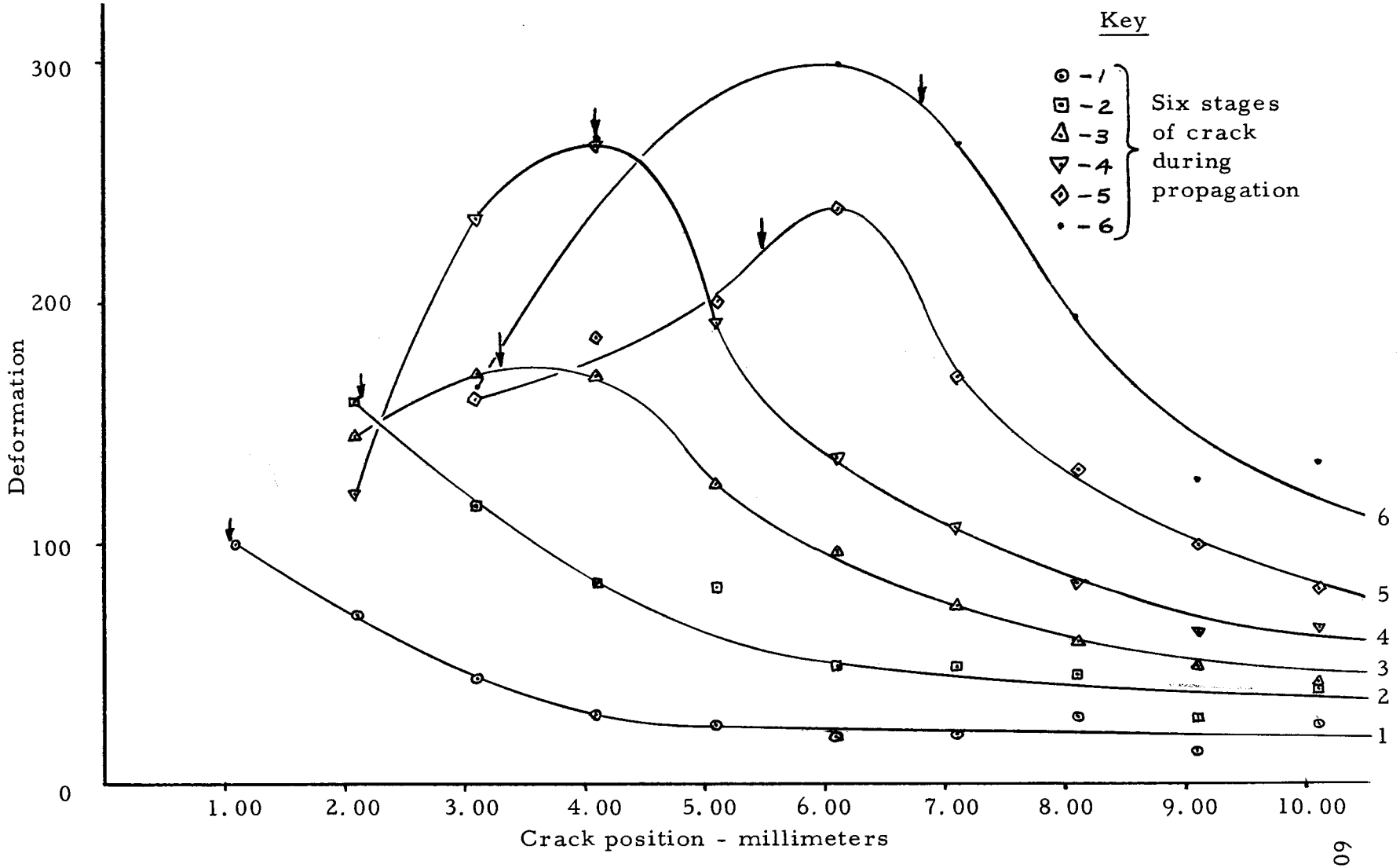

Fig. 17. Variation of Deformation with Crack Position for Various Stages of Crack Growth.

of strain present and it will be noticed that as one approaches the vicinity of the crack the strain gradient increases as does the actual strain.

Curve three begins to assume the shape of the stable configuration of strain gradient. There is a general increase in the strain over the whole surface of the specimen with an abrupt rise in the strain immediately ahead of the crack. The decrease in the strain after the crack has passed is shown here and the reasons for this have already been associated with the effects of elastic recovery.

Curves four, five, and six all show the same general configuration of strain gradient. Due to the extensive length of time necessary to record all the data it is possible that there was some creep occurring in the specimen. This would help explain the higher maximum in curve four than the maximum value of curve five since the data were taken on different days. Another factor which would contribute to this discrepancy in the data is the fact that the process of propagation is not smooth, in that the crack tends to progress in steps and may not follow a regular path. As the stress is increased a crack will jump ahead and then stop and then will jump again. This steplike movement of the crack on an irregular path would be expected to produce an irregular or steplike variation in the strain gradient. This would lead to a range of values of strain that could be observed depending on the condition of the crack at the instant that the data is

taken.

The data from these tests corroborate the previous observations, discussed in connection with the photomicrographs, that extensive plastic deformation is occurring throughout the specimen. The abrupt rise in each curve ahead of the crack tip shows that there is a region in which large, but localized deformations are occurring and it also supports the assumption that the maximum strain is occurring near the tip of the crack. However, the gradual decrease in the strain ordinate ahead of the crack indicates that the plastic strain shown in Figure 17 tapers off as the distance from the crack increases and it seems apparent that this decrease in plastic strain continues to the boundaries of the specimen.

On the basis of the photomicrographs and the deformation measurements that were made it is not possible to either support or criticize the theory of slow crack propagation. During the initial stages of crack growth it is apparent that the plastic deformation is spreading throughout the whole volume of the specimen. However, the measurements that were made were not sufficient to describe the plastic deformation effects at a position which is a large distance from the crack tip. Therefore, it has been shown that the plastic deformation does not appear to be confined to a given geometrical configuration and that it does progress outwards from the crack tip during the initial stages of crack growth. It is not possible, however,

to determine, on the basis of the data obtained, whether this plastic deformation continues to grow outwards as the crack continues to grow or whether it attains a stable configuration which moves along with the crack.

Further analysis of the data obtained from the second series of tests is possible by calculating the actual strains which occurred between each pair of indentations. This was done by finding the amount of deformation which occurred between each of the pairs of adjacent indentations which make up the eleven sets of indentations. This calculation was made for the data of curves four, five, and six since they all show nearly the same configuration. The calculations and resultant data are shown in the Appendix. The total strains, including both elastic and plastic components, were then calculated from the deformations and are averaged for the three curves at equivalent positions relative to the crack tip. The eight indentations in each of the eleven sets separate the material adjacent to the crack into seven rectangular strips parallel to the crack as seen in Figure 12. Seven curves were then plotted from the data which represent the variation of strain with distance from the crack tip, in the direction that the crack was running, for each of the seven strips of material. These curves are shown in Figure 18.

An iso-strain contour may be drawn around the crack tip by picking a value of constant strain and noting the distances from the

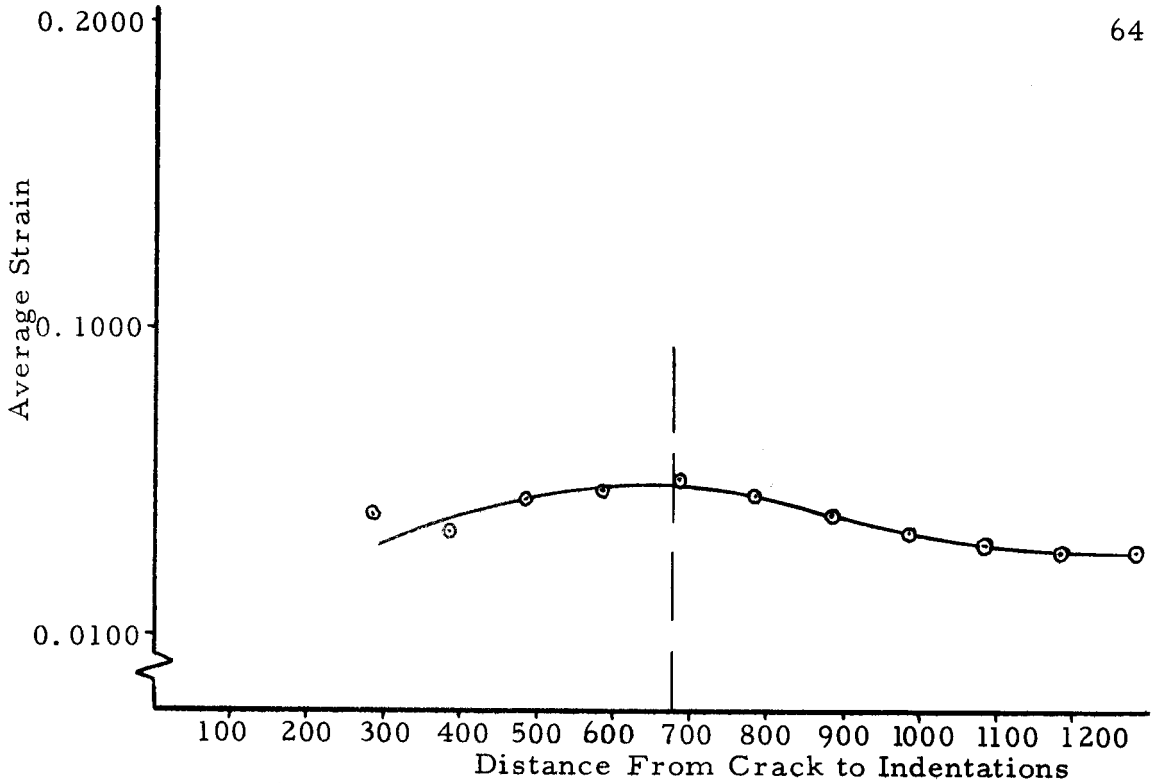

Fig. 18b. Average Strain Versus Indentation Position Relative to the Crack Tip Position "B".

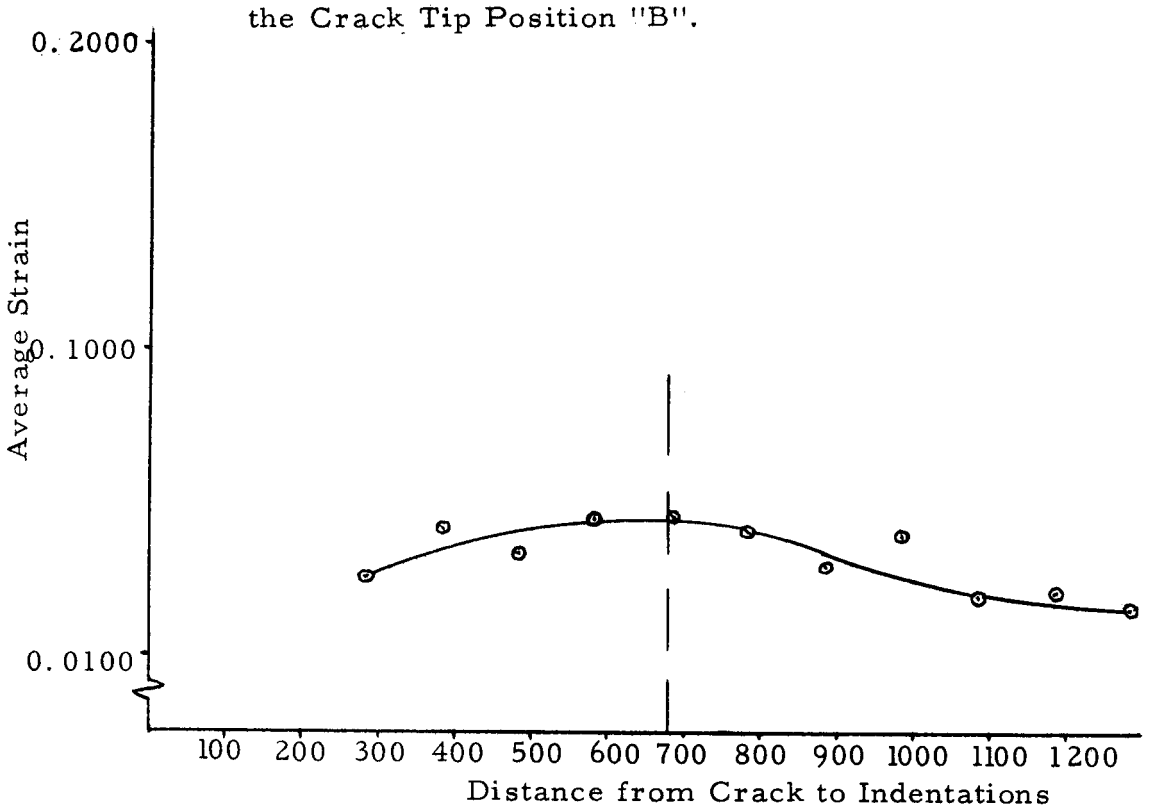

Fig. 18a. Average Strain Versus Indentation Position Relative to the Crack Tip Position "A".

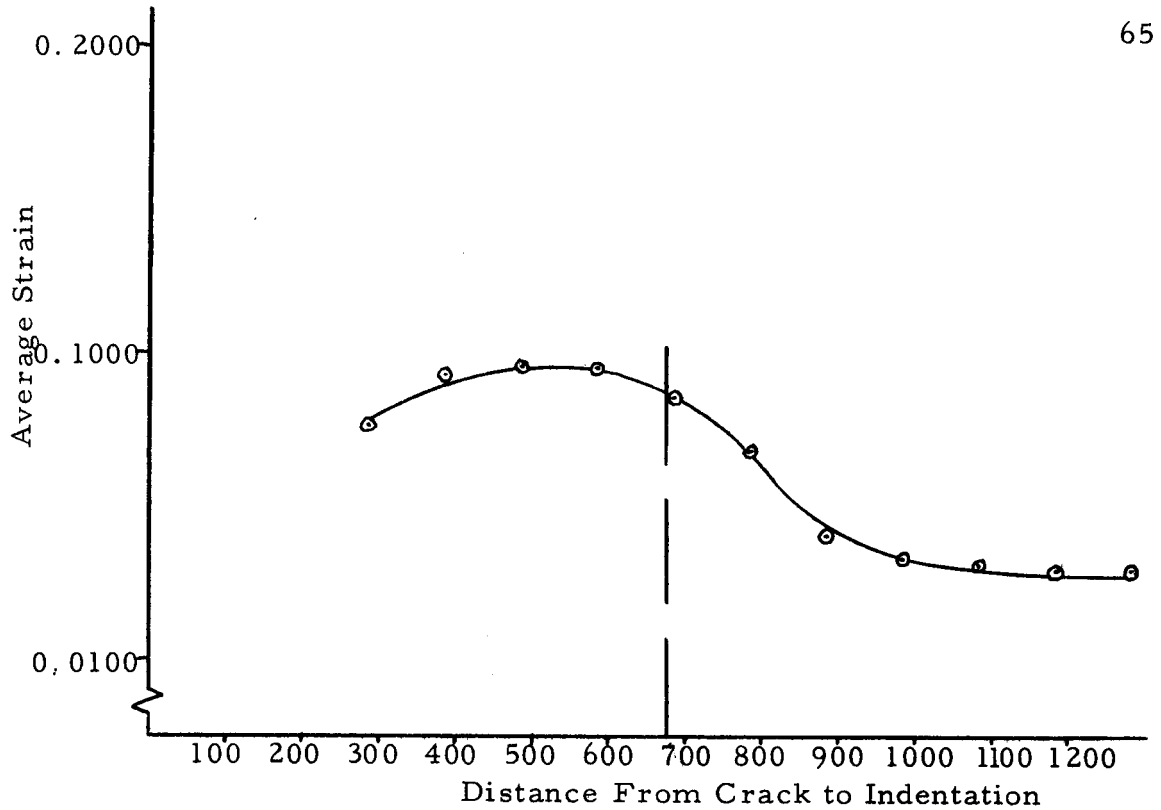

Fig. 18d. Average Strain Versus Indentation Position Relative to the Crack Tip Position "D".

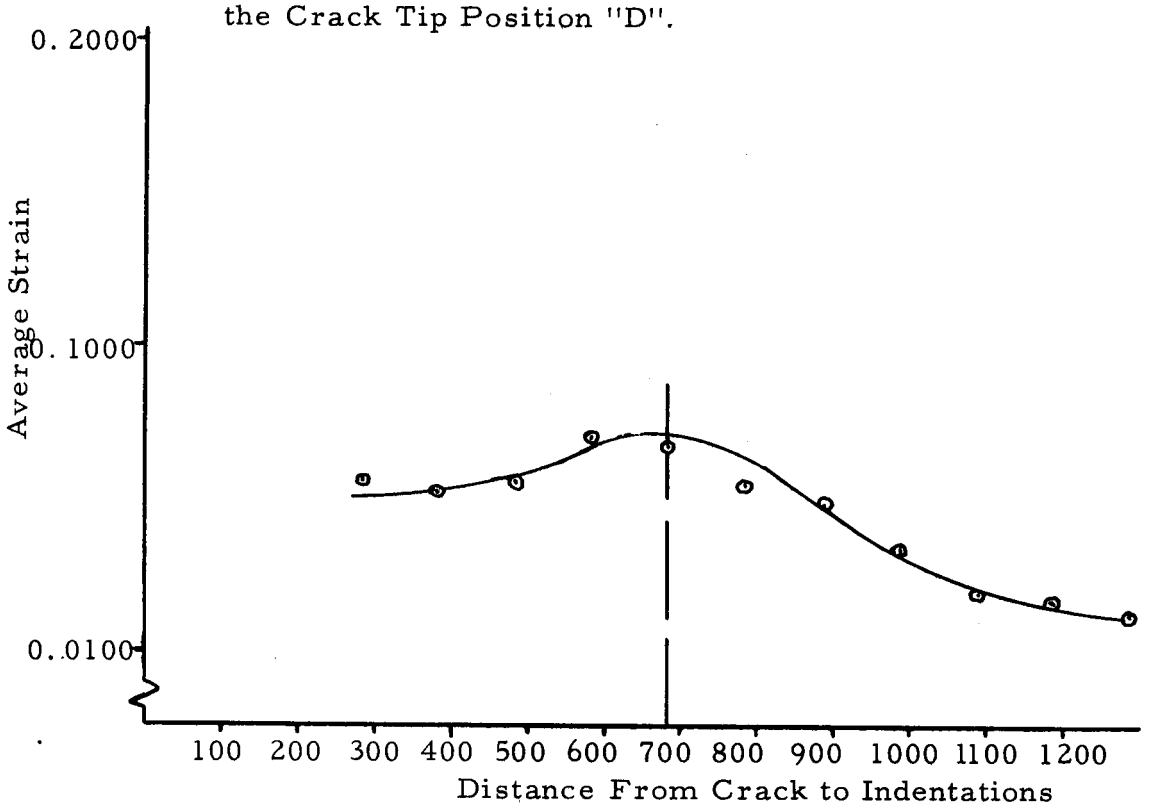

Fig. 18c. Average Strain Versus Indentation Position Relative to the Crack Tip Position "C".

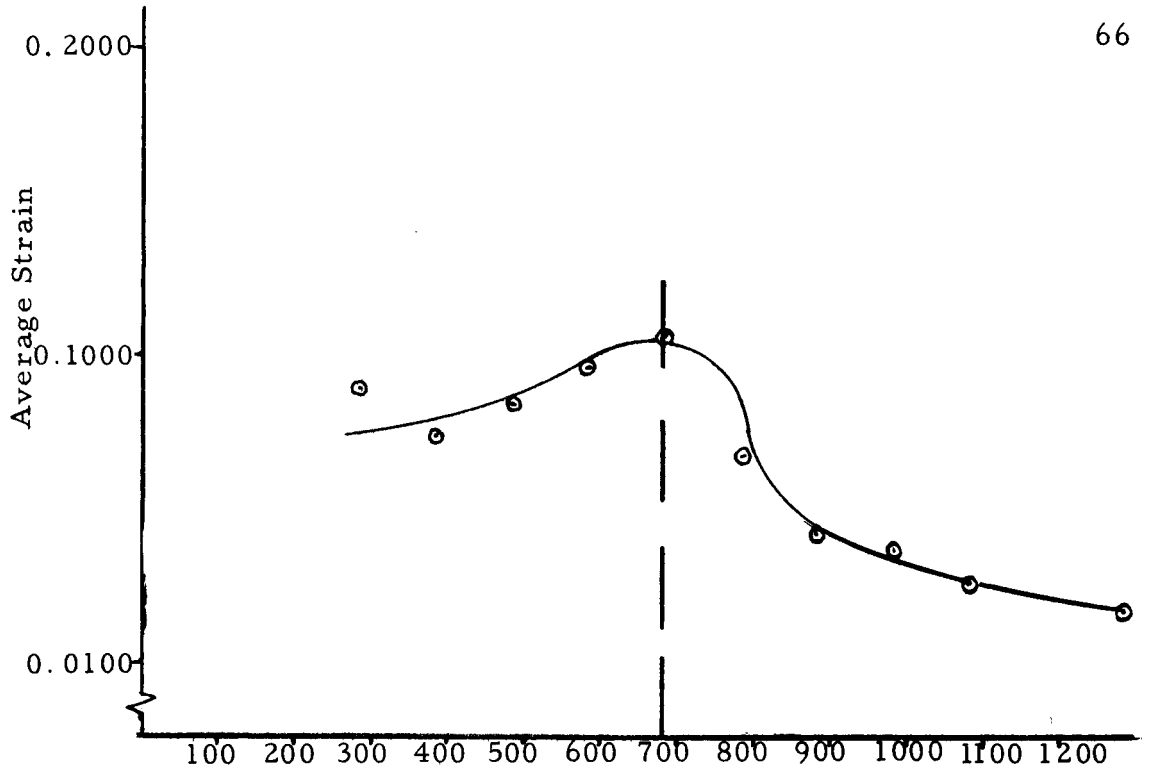

Fig. 18f. Average Strain Versus Indentation Position Relative to the Crack Tip Position "F".

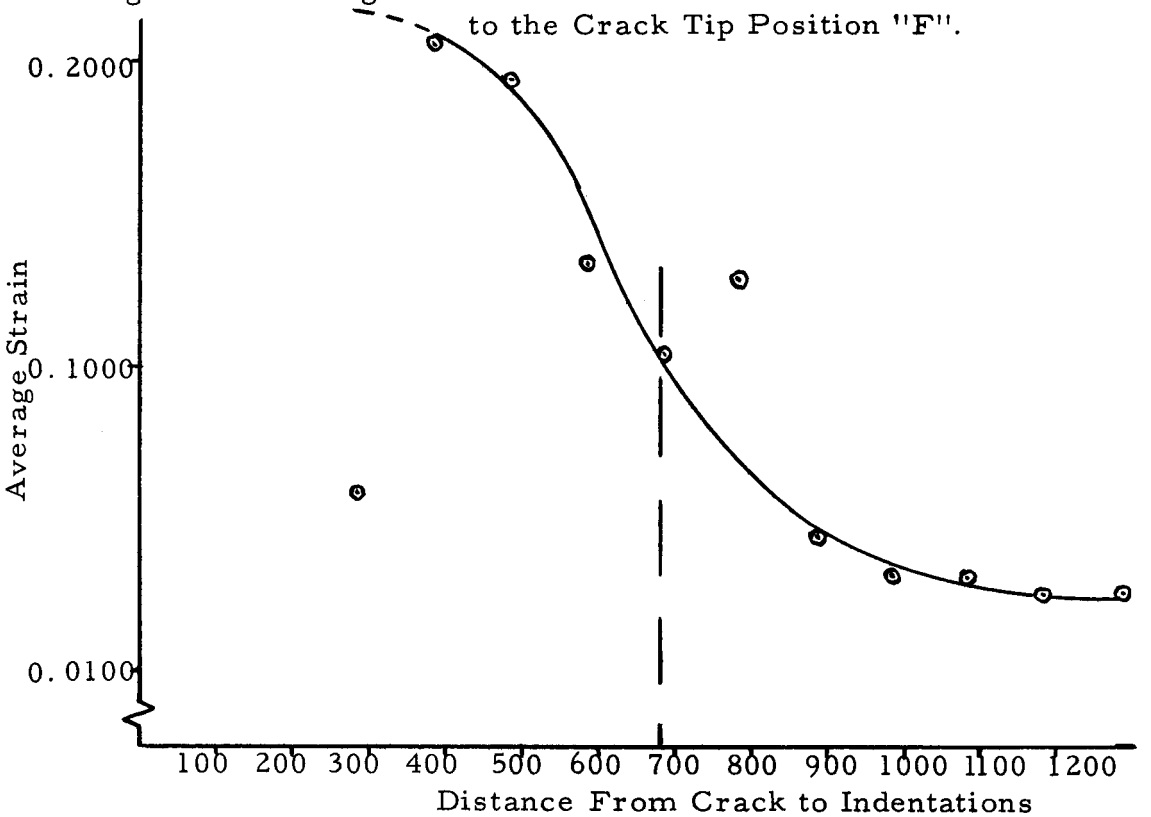

Fig. 18e. Average Strain Versus Indentation Position Relative to Crack Tip Position "E".

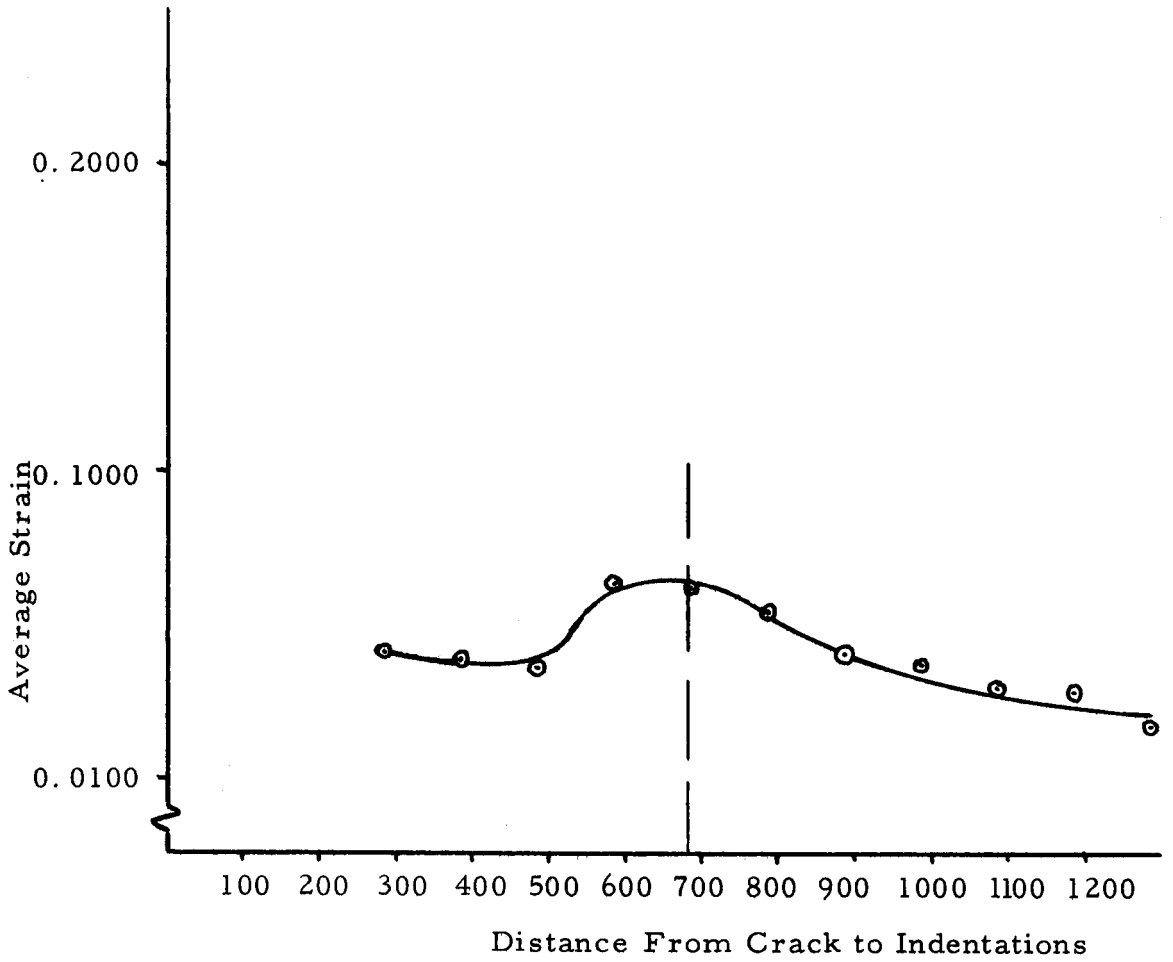

Fig. 18g. Average Strain Versus Indentation Position Relative to the Crack Tip Position "G".

crack tip at which this value of strain occurs for each of the seven curves shown in Figure 18. These data were plotted and the resulting map of iso-strain contours is shown in Figure 19. In order to make a more complete map it would be necessary to use a greater number of indentations and place them closer together. This would entail the expenditure of a great deal of time and work.

The iso-strain contours shown are based on a limited amount of data and several assumptions and approximations were made in completing them. The data, however, indicated the general shape of the complete curves for some of the contours and the rest of the contours were drawn in similarly. In order to avoid misinterpretation of the iso-strain curves it should be noticed that there is a difference in the scales on the horizontal and vertical axes.

Figure 19 indicates the distribution of strains around the tip of a propagating crack in which the strains have assumed a stable configuration. The contour lines are nearly symmetrical around the crack tip except for the lower portions of the curves in the strain relieved area. The spacing between the lines of constant strain in this area are much smaller than the spacing between corresponding strain lines in the upper portion of the map. No logical explanation is readily available but it is very likely due to the inherent irregularity in the deformation and crack propagation process, which cause irregularities in the data. As has been previously mentioned, the

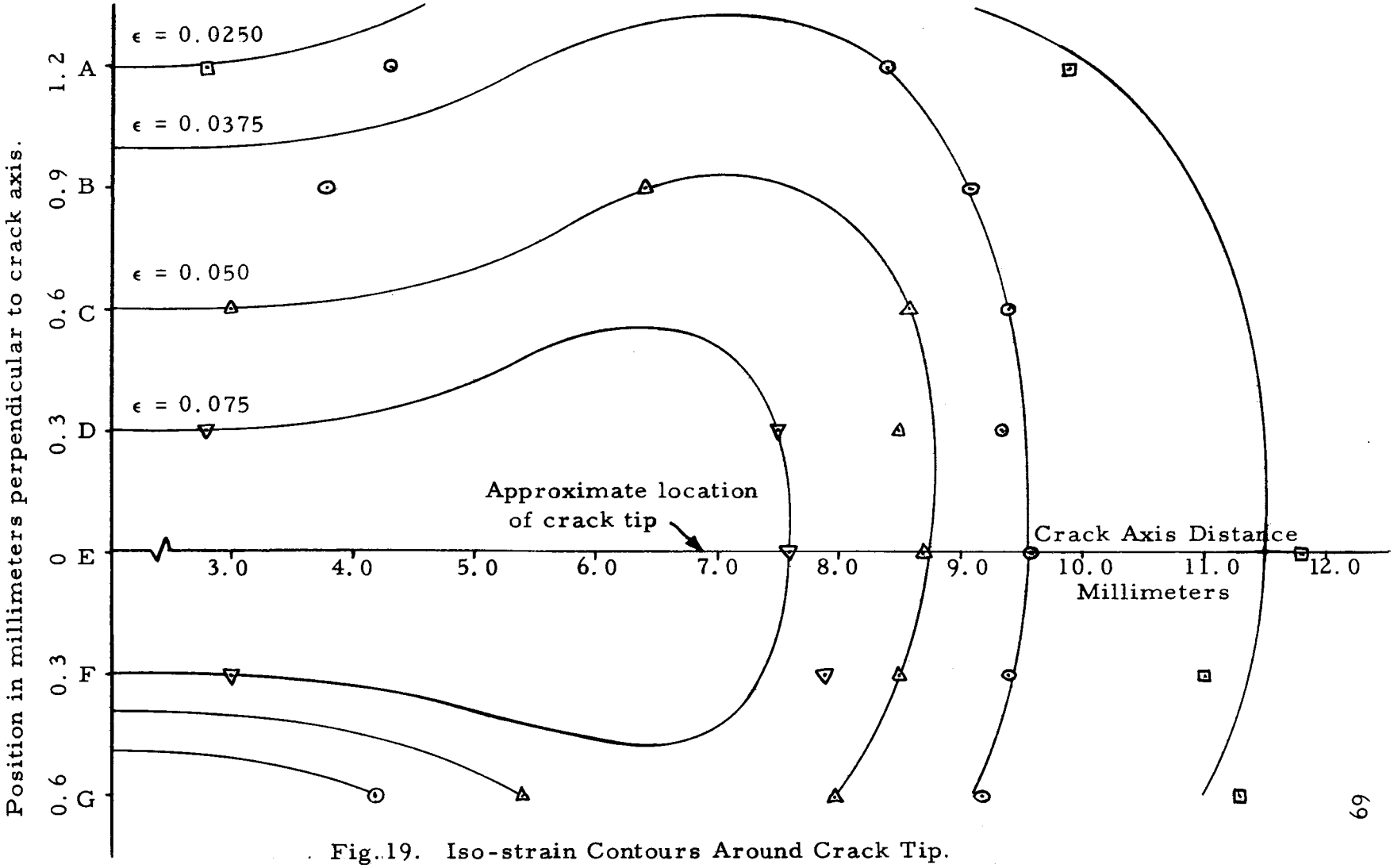

Fig. 19. Iso-strain Contours Around Crack Tip.

propagation of a crack is a very irregular process and this leads to scatter in the data that are obtained. Therefore, after the calculations are made and the data points are obtained from the plotted curves it is probable that some erratic effects have accumulated.

The effects of elastic recovery are obviously here as indicated by the fact that the contours of higher constant strain at any given crack position move closer to the crack axis after the crack tip has passed that position. The strain in the rounded portions of the curves around the crack tip are total values which include both elastic and plastic strain. In the strain relieved area, however, the elastic part of the strain is not present and only the plastic strain remains which is indicated by the level portions of the curves near the origins of the crack. It is not possible, however, to determine the relative proportions of the elastic and the plastic strain in the areas surrounding the crack.

Using the data and the curves of Figure 19 it is possible to make an approximation of the length of crack that would be necessary in order to cause the crack to propagate catastrophically. It will be recalled that the criterion for rapid crack growth was that the release of strain energy must equal or exceed the work done in plastically deforming the material for unit changes in the crack length. This was stated symbolically:

$$\frac{dG}{dA} \geq \frac{dP}{dA}$$

The amount of plastic work that has been done may be calculated from the values of the iso-strain contours and the stress-strain diagram for the material. This was done and the calculations are shown in the Appendix. This value for the plastic work done can then be equated to the expression for the strain energy in the material which was:

$$\frac{dG}{dA} = \frac{\sigma^2 K_1 \ell}{2E}$$

Assuming a value of stress of 5000 psi, which is close to the stress values used in some of the unsuccessful tests run during phases one and two of the project, the length of crack necessary for rapid crack growth to occur may be calculated. This value was found to be 48.7 inches, assuming the case of infinite boundaries. Obviously, a crack length of this magnitude was not obtainable on the equipment used and this would help explain the failure to obtain catastrophic crack propagation at this low value of stress. This is, of course, a rough approximation although an error of even 50 percent would not change the significance of the final answer.

If the calculations are correct, no catastrophic failure should take place under the assumed testing conditions. However, as was mentioned previously, this type of failure was observed during the first two phases of the testing program. The most logical explanation

of this occurrence is that the testing conditions did not completely satisfy the several assumptions upon which the theory was based. This would include the fact that work was done on the system even though precautions were taken to prevent this. The occurrence of unaccounted-for strain such as due to creep or slippage of the foil in the clamps would cause a variation from theoretical conditions. Energy might also have been received from the foam rubber in the clamps since deformation of the rubber occurred during the stressing of the foil.

The movement of the boundaries and the resulting work on the system probably are the greatest cause of the occurrence of catastrophic propagation which would account for the variation of the experimental results from those predicted on the basis of the theory. The crack lengths calculated previously are much too large to satisfy the theoretical assumption that the crack length is small in comparison to the width of the sheet. The case of infinite boundaries was used for the calculations and much larger sheets of foil would be needed to comply with this assumption.

In future testing programs the problem could be avoided by using a material which has been work hardened so that the amount of energy absorbed in plastic deformation would be less. This would allow criticality to occur at much shorter crack lengths than those calculated although the stresses needed would be higher. For these

tests it might be advisable to use thin sheets of the material rather than a foil. This would decrease the problems in handling the specimens although it would require the construction of a larger testing apparatus. Once the necessary conditions for criticality have been established an investigation of the effects of metallurgical variables on the tendency for a crack to propagate catastrophically in a given material can be made.

CONCLUSIONS

1. The plastic deformation at the tip of the crack was not observed to be confined to a given geometrical area.
2. A regular symetrical pattern of iso-strain contours was observed to exist around the tip of a propagating crack.
3. The phenomenon of slow crack propagation was observed in the second phase of testing although no definite supporting data for the theory of slow crack growth were obtained.
4. The maximum amount of strain was observed to occur in the material adjacent to the crack tip and a decrease in the strain was seen to occur as the crack progressed past the point in question.
5. Calculations based on the theory showed that the critical crack length at which catastrophic propagation could occur would be much larger than was obtainable with the available equipment. The fact that catastrophic failure was observed was attributed to the fact that the testing conditions did not satisfy the theoretical assumptions made.
6. Further experimentation in the areas of slow crack growth and plastic deformation effects at the crack tip is needed to provide the data necessary for more complete understanding of these phenomena.

7. Further experiments on catastrophic propagation could be improved by using work hardened material in sheet form.

BIBLIOGRAPHY

1. American Society for Testing Materials Special Committee. Fracture testing of high strength sheet materials, 1960. p. 29-40. (American Society for Testing Materials Bulletin no. 243.)

2. American Society for Testing Materials Special Committee. Fracture testing of high strength sheet materials, 1960. p. 18-28. (American Society for Testing Materials Bulletin no. 244.)

3. American Society for Testing Materials Special Committee. The slow growth and rapid propagation of cracks. Materials Research and Standards 1: 389-393. 1961.

4. Averbach, B. L., D. K. Felbeck, G. T Hahn and D. A. Thomas (eds.) Fracture. Proceedings of an International Conference on the Atomic Mechanisms of Fracture Held at Swampscott, Massachusetts, John Wiley and Sons, Inc., 1959. 646 p.

5. Chalmers, Bruce. Physical metallurgy. New York, John Wiley and Sons, Inc., 1959. 468 p.

6. Corten, Herbert T. and Ford R. Park. Fracture. International Science and Technology no. 15: 24-36. March 1963.

7. Erdogan, Fazil, O. Tuncel and P. C. Paris. An experimental investigation of the crack tip stress intensity factors in plates under cylindrical bending. Journal of Basic Engineering 84: 542-546. December 1962.

8. Griffith, A. A. The phenomena of flow and rupture in solids. Philisophical Transactions of the Roy Society of London A221: 163-198. 1921.

9. McClintock, F. A. Ductile fracture instability in shear. Journal of Applied Mechanics 80: 582-588. 1958.

10. McClintock, F. A. On the plasticity of the growth of fatigue cracks. Cambridge, Massachusetts Institute of Technology, n. d. 39 p.

11. Olleman, R. D. A tensile study of temper brittleness in SAE 3335 steel at temperatures from 25 C to -269 C. Ph. D. Thesis. Pittsburg, University of Pittsburg 1955. 208 numb. leaves.

12. Omelka, L. V. and D. A. Paul. Typical stress-strain and tangent modulus curves for Kaiser aluminum alloys. Spokane, 1954. 41 numb. leaves. (Kaiser Aluminum and Chemical Corporation. Research Bulletin no. 1.)

13. Orowan, E. Energy criteria of fracture. Welding Research Supplement 34: 157-s -- 160-s. March 1955.

14. Paris, P. C. The initiation, propagation, and arrest of fractures in aircraft metals. Seattle, 1955. (Boeing Airplane Company. Structural Development Note no. 45.)

15. Sih, G. C., P. C. Paris and F. Erdogan. Crack tip stress intensity factors for plane extension and plane bending problems. Journal of Applied Mechanics 84: 306-312. 1962.

16. White, F. M. On fracture in thin metallic sheets. Master's Thesis. Cambridge, Massachusetts Institute of Technology, 1956. 48 numb. leaves. (Microfilm)

17. Zener, C. The micro-mechanism of fracture. In: Fracture of metals. Cleveland, American Society for Metals, 1948. p. 3-31.

APPENDIX

SAMPLE CALCULATIONS FOR PLASTIC DEFORMATION TESTS SERIES I AND II

Series I Calculations

The data necessary for the analysis of these tests were the crack to indentation distances and the deformation of the material between the indentations. The crack to indentation distances were read directly from the micrometer screw on the microton and the deformations were calculated from the positions of the indentations. The raw data is shown in Table I. The indentations were numbered one through six and the position of each indentation was measured for each crack position. The distances between adjacent indentations were calculated by taking the differences in the position measurements. These differences were designated as A, B, C, and so on. Therefore:

$D_2 - D_1 = A$

$D_3 - D_2 = B$

. . . . .

Where: D is the position of the various indentations.

The deflections for each spacing at the various crack positions were found by taking the difference between the initial distance between two adjacent indentations and the final distance between the same two indentations. Therefore:

$A_2 - A_1 = \delta_A$

$B_2 - B_1 = \delta_B$

. . . . .

Where: δ is the deflection in the individual spaces.

Table I. Raw Data for Plastic Deformation Measurements - Series I.

l_c	l_s	L	1	2	3	4	5	6
044	1160	1116	943	522	086			
					941	324		
						907	486	052
066	1156	1090	923	500	062			
					741	119		
						945	519	082
174	1151	977	934	509	071			
					718	094		
						918	492	053
258	1144	886	925	501	060			
					957	332		
						927	499	057
336	1090	754	922	494	055			
					903	276		
						896	467	027
508	1035	527	936	509	063			
					958	326		
						952	521	077
646	979	333	953	517	068			
					964	527		
						956	520	069
759	924	165	960	520	060			
					968	319		
						959	517	061
821	921	100	965	518	045			
					943	264		
						942	485	019
891	919	28	978	529	056			
					965	239		
						960	503	033
919	919	0	960	513	041			
					959	216		
						951	492	022
1015	916	-99	935	492	020			
					965	134		
						956	498	028

Table II. Calculated Deflections for Plastic Deformation Tests - Series I.

L	A	B	C	D	E
1090	2	2	4	5	3
977	2	0	2	0	2
886	-1	3	1	2	3
954	4	-2	2	1	-2
527	-1	7	5	2	4
333	9	3	5	5	7
165	4	11	12	6	5
100	6	13	30	15	10
28	2	0	47	0	4
0	02	01	17	2	0
-99	-4	0	88	01	0

Series II Calculations

The raw data for the Series II tests was similar to the data for the Series I tests except that there were eleven sets of eight indentations in the second tests. The differences in the indentation positions were calculated as in Series I. However, the total elongation of the complete set of points was calculated instead of the individual deflections. This was accomplished by obtaining the sums of the differences for each set of indentations. These sums were then corrected for the elongation due to the crack passing between the indentations. The corrected values were checked by actually measuring the width of the crack during the tests. The calculated differences are shown in Table III and the total deflections are shown in Table IV.

Iso-Strain Contour Calculations

The data for the iso-strain contour map was calculated by taking the deflections for each of the individual spaces between the spots in sets four, five, and six of the Series II tests in a manner similar to that used in the Series I calculations. These deflections were then divided by the original distance between the indentations for each space to obtain the strain occurring in that space. These strain values were then averaged for the three sets of data for corresponding spaces and these values are shown in Table V. The average strain values were plotted versus the crack distance for each of the seven

Table III. Raw Data and Calculated Differences for Plastic Deformation Tests.
Series II Set I

L_c	L_s	1	A	2	B	3	C	4	D	5	E	6	F	7	G	8
070	110	931	423	508	437	071										
						921	422	499	428	071						
										921	434	487	425	062		
														502	440	062
070	933	933	423	510	438	072										
						928	423	505	433	072						
										928	430	498	426	072		
														503	431	072
070	310	953	422	531	436	095										
						955	427	528	433	095						
										955	429	526	426	100		
														538	438	100
070	410	942	423	519	437	082										
						938	425	513	431	082						
										938	432	506	425	081		
														513	432	081
070	510	939	424	515	433	082										
						933	422	511	429	082						
										933	432	501	425	076		
														515	439	076
070	610	939	425	514	435	079										
						935	421	514	435	079						
										935	431	504	425	079		
														512	433	079
070	710	924	423	501	436	065										
						919	422	497	432	065						
										919	426	493	426	067		
														495	428	067
070	810	936	423	513	436	077										
						932	423	509	432	077						
										932	433	499	424	075		
														495	420	075
070	910	957	429	538	436	102										
						955	421	534	432	102						
										955	428	527	430	097		
														525	428	097
070	1010	920	424	496	436	060										
						915	425	490	430	060						
										915	437	478	423	055		
														479	424	055
070	1110	959	416	543	437	106										
						961	427	534	428	106						
										961	431	530	427	103		
														530	427	103

Table IV. Calculated and Corrected Values of Total Deformation for Plastic Deformation Tests - Series II.

Set	1	2	3	4	5	6	7	8	9	10	11
1	3009	3004	3011	3005	3004	3005	2993	2991	3004	2999	2993
2	3108	3075	3054	3033	3029	3024	3014	3018	3017	3023	3012
3	--	3162	3127	3089	3096	3054	3041	3036	3031	3037	3029
4	--	3149	3181	3179	3129	3101	3067	3049	3052	3041	3039
5	--	3125	3246	3271	3196	3141	3100	3074	3067	3063	3054
6	--	--	3171	3191	3205	3244	3162	3121	3103	3080	3067
7	--	--	3177	3275	3273	3304	3259	3185	3131	3132	3093

Calculated Differences in Deformation for Plastic Deformation Test - Series II.

Set	1	2	3	4	5	6	7	8	9	10	11
1											
	99	71	43	228	25	19	21	27	13	24	19
2											
	--	158	116	84	82	49	48	45	27	38	36
3											
	--	145	170	169	125	96	74	58	48	42	46
4											
	--	121	235	266	192	236	207	83	63	64	61
5											
	--	--	160	186	201	239	169	130	99	81	70
6											
	--	--	166	270	269	299	266	194	127	133	100
7											

Table V. Average Strains - Sets 5, 6, & 7.

A	B	C	D	E	F	G
-	-	-	-	-	-	-
-	-	-	-	-	-	-
.0262	.0390	.0561	.0762	.0582	.8093	.0411
.0422	.0331	.0514	.0936	.2058	.0733	.0385
.0339	.0445	.0542	.0960	.1927	.0837	.0356
.0448	.0475	.0695	.0951	.1332	.0956	.0630
.0456	.0503	.0656	.0856	.1033	.1059	.0617
.0417	.0452	.0529	.0678	.1282	.0659	.0538
.0282	.0398	.0466	.0407	.0435	.0411	.0400
.0393	.0333	.0323	.0332	.0308	.0361	.0370
.0183	.0321	.0189	.0318	.0301	.0255	.0289
.0214	.0275	.0165	.0292	.0254	———	.0271
.0168	.0275	.0117	.0280	.0255	.0164	.0164

spaces and from these curves the positions of the points of constant strain could be determined. These values are shown in Table VI and were plotted versus crack position to obtain the map of iso-strain contours.

Table VI. Iso-Strain Contour Data.

Strain	Position	Distance	
0.0250	A	280	990
"	E	-	1180
"	F	-	1100
"	G	-	1130
0.0375	A	430	840
"	B	380	910
"	C	-	940
"	D	-	935
"	E	-	960
"	F	-	940
"	G	420	920
0.0500	B	-	640
"	C	300	860
"	D	-	850
"	E	-	870
"	F	-	850
"	G	540	800
0.075	D	280	750
"	E	-	760
"	F	300	790

PLASTIC DEFORMATION ENERGY CALCULATIONS

The plastic strain energy for each of the strips parallel to the crack may be calculated by assuming an average value for the strain in the strip. In Figure 19 the iso-strain contours near the letters A, B, C, and D are used to divide the material adjacent to the crack into four nearly equal strips. The average strain in each strip is found by averaging the strain on the adjacent contours.

The amount of plastic strain energy is found by taking the area under the stress-strain curve for 1100-H14 Aluminum up to the particular value of strain for the strip being considered. This procedure is done for each of the four strips. The area of each strip per unit length of crack is:

$$\text{Area} = \frac{(0.3 \text{ mm})\,(1 \text{ in.})\,(0.001 \text{ in.})}{(25.4 \text{ mm/in.})} = 1.18 \times 10^{-5} \text{ in.}^2$$

For both sides of the crack:

$$\text{Area} = 2.36 \times 10^{-5} \text{ in.}^2$$

The strain energy in each strip per unit length of crack may now be calculated by taking the values obtained from the area under the curve and multiplying this by the area of the strip per unit length of crack.

Or: Strain Energy = (2.36×10^{-5}) (Area under Curve)

The total strain energy in all four strips on each side of the crack is found by adding the individual strain energy values together.

In order to have an instable crack, it was shown in the theory that:

$$\frac{dP}{dA} = \frac{dG}{dA}$$

and dG/dA is given by:

$$\frac{dG}{dA} = \frac{\sigma^2 K_1 \ell}{2E}$$

Multiplying this by the thickness "t" the expression can be put on the basis of a unit of crack length. Therefore, we have:

$$\text{Strain Energy} = \frac{t\sigma^2 K_1 \ell}{2E}$$

The calculated value of the strain energy was:

$$\text{Strain Energy} = 0.0955 \text{ in lb/in}$$

and the thickness of the foil was 0.001 inches.

Therefore:

$$0.0955 = \frac{(0.001)(\sigma^2 K_1 \ell)}{2E}$$

Assuming that the stress is 5000 psi, the critical length of the crack is found to be:

$$\ell = 48.7 \text{ inches}$$